

CERN-EP-2024-299

13 November 2024

Observation of partonic flow in proton–proton and proton–nucleus collisions

ALICE Collaboration*

Abstract

Quantum Chromodynamics predicts a phase transition from ordinary hadronic matter to the quark–gluon plasma (QGP) at high temperatures and energy densities, where quarks and gluons (partons) are not confined within hadrons. The QGP is generated in ultrarelativistic heavy-ion collisions. Anisotropic flow coefficients, quantifying the anisotropic azimuthal expansion of the produced matter, provide a unique tool to unravel QGP properties. Flow measurements in high-energy heavy-ion collisions show a distinctive grouping of anisotropic flow for baryons and mesons at intermediate transverse momentum, a feature associated with flow being imparted at the quark level, confirming the existence of the QGP. The observation of QGP-like features in relativistic proton–proton and proton–ion collisions has sparked debate about possible QGP formation in smaller collision systems, which remains unresolved. In this article, we demonstrate for the first time the distinctive grouping of anisotropic flow for baryons and mesons in high-multiplicity proton–lead and proton–proton collisions at the Large Hadron Collider (LHC). These results are described by a model that includes hydrodynamic flow followed by hadron formation via quark coalescence, replicating features observed in heavy-ion collisions. This observation is consistent with the formation of a partonic flowing system in proton–proton and proton–lead collisions at the LHC.

Ultrarelativistic collisions of heavy ions at the Relativistic Heavy Ion Collider (RHIC) and the Large Hadron Collider (LHC) create the quark–gluon plasma (QGP), a short-lived state of strongly interacting partonic matter, thought to have existed a few microseconds after the Big Bang [1]. The interactions among partons in the QGP, combined with the initial spatial anisotropy of the overlap region of colliding ions, create anisotropic pressure gradients in the transverse plane of the collision. These anisotropic pressure gradients result in momentum anisotropy of the emitted particles [2]. The anisotropic particle emission is quantified using the Fourier decomposition of the azimuthal distribution of the final state particles [3]

$$\frac{dN}{d\phi} \propto 1 + \sum_n 2v_n(p_T) \cos(n\phi - n\Psi_n). \quad (1)$$

Here, ϕ and p_T denote the azimuthal angle and transverse momentum of the emitted particles, respectively, while Ψ_n is the azimuthal angle of the symmetry plane for the n -th harmonic. The largest contributions are the second and third Fourier coefficients, namely elliptic (v_2) and triangular (v_3) flow [4–6], which result from the elliptic and triangular shapes in the initial overlap region of the colliding nuclei. The anisotropic flow extends along pseudorapidity ($\eta \equiv -\ln(\tan \frac{\theta}{2})$), where θ is the polar angle of the particle), forming an elongated structure known as the ridge [7]. In heavy-ion collisions, precise measurements of v_n [4, 6, 8, 9] and detailed comparisons with models employing relativistic viscous hydrodynamics reveal that the QGP behaves as a liquid with viscosity to entropy density ratio close to the lowest theoretical value allowed [10, 11].

In high-energy heavy-ion collisions, the v_2 coefficient of identified hadrons exhibits a characteristic mass dependence at low p_T , meaning that more massive particles show lower v_2 values at a given p_T [12–14]. Mass ordering arises from the interplay between average radial expansion velocity, anisotropic flow velocity, and thermal motion, which pushes heavier particles to higher p_T [15, 16]. This results in a mass-dependent reduction in v_2 at low p_T ($p_T < 3.0$ GeV/ c). In the intermediate p_T region ($3.0 < p_T < 8.0$ GeV/ c), a clear separation between the flow patterns of baryons (hadrons composed of three quarks or three antiquarks) and mesons (hadrons composed of quark–antiquark pairs) is observed with $v_2^{\text{baryons}} > v_2^{\text{mesons}}$ [14, 17, 18]. A physical process that can explain this distinctive grouping of hadron v_2 based on their valence quark number is hadron formation via quark coalescence [19]. In this process, a meson (baryon) is formed by combining two (three) quarks, and the meson (baryon) v_2 is obtained by combining the v_2 values of the two (three) quarks, as illustrated in Fig. 1. The experimental observation of baryon-meson grouping at intermediate p_T is therefore interpreted as a consequence of a medium that includes a phase with collectively flowing partons.

Proton–proton and proton–nucleus collisions were used as a baseline to study the QGP in heavy-ion collisions at RHIC and the LHC, as QGP formation was not expected in small collision systems. However, striking similarities have been observed between numerous observables in both small collision systems and heavy-ion collisions at RHIC and LHC energies. These observables include the ridge [20–23], mass dependence of v_2 at low p_T [21, 24, 25], azimuthal angle correlations carried by multiple particles [26], and strangeness and baryon enhancement with increasing multiplicity [27]. These features are commonly considered indicators of QGP formation. The standard picture in heavy-ion collisions is that anisotropic flow is built up after the collision through final-state interactions among the partons combined with the initial spatial anisotropy of the overlap region of the colliding nuclei. In small collision systems, where the system evolution is shorter than in heavy-ion collisions and a QGP phase is not expected, a different scenario is proposed within the framework of Color Glass Condensate (CGC) effective theory [28]. According to this theory, the observed flow patterns come from the initial gluon momentum correlations in the colliding hadrons. These gluons scatter off specific regions, or color domains, during the collision and get a momentum boost in the same direction if they scatter from the same color domain. The current understanding is that initial-state momentum anisotropy alone cannot explain the existing data, and the measurements seem to favor the scenario of final-state effects driven by initial geometry [1, 23], following a similar scenario as in heavy-ion collisions. However, the impact of initial gluon momentum

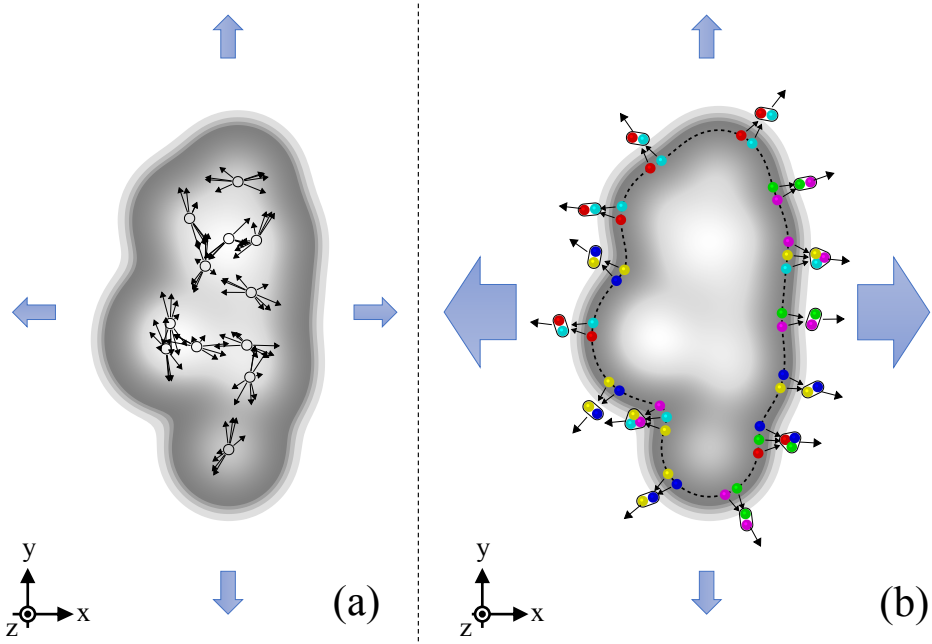


Figure 1: A schematic representation of the overlap region in a collision is shown in gray, along with overall particle emission patterns in the transverse (x-y) plane, represented by large arrows. a) Non-flow sources: These are independent emissions, such as those from resonance decays or jets, where jets are collimated streams of hadrons created when a high-energy quark or gluon fragments after a collision. These effects lead to few-particle correlations but are not related to collective behavior in the system and have been subtracted from the final anisotropic flow measurements (see methods subsection A.4 for details). b) Anisotropic flow: This illustrates the development of anisotropic flow in a partonic system, propagated to the level of hadrons via the quark coalescence process, which describes the experimental measurements in the intermediate p_T range ($\sim 3\text{--}8 \text{ GeV}/c$). In this process, two or three flowing partons coalesce to form mesons or baryons, which then interact with each other. The large arrows represent the overall anisotropy of particle emission in the transverse plane, with stronger expansion along the short (x) axis.

correlations on the development of anisotropic flow in small collision systems is not clear yet. At the same time, the precise mechanisms underlying the final-state effects remain unclear. The flow can develop during a partonic phase, transforming the initial spatial anisotropy into the measured flow [29–34], or it can originate via other mechanisms without the need for a deconfined phase, such as rescatterings among hadrons [35], via approaches involving initial state effects [36], or via different string dynamics implemented in the PYTHIA 8 event generator [37]. None of the measurements performed so far have been able to give a clear answer to this question.

This work takes a step further in resolving the puzzle of the origin of collective flow in small collision systems by investigating the possibility of a partonic phase and its role in the system’s dynamic evolution. Utilizing the unique particle identification capabilities of the ALICE detector at the LHC [38, 39], the elliptic flow (v_2) as a function of p_T is presented for mesons (π^\pm, K^\pm, K_S^0) and baryons ($p+\bar{p}, \Lambda+\bar{\Lambda}$) in pp and p-Pb collisions at a nucleon–nucleon center-of-mass energy ($\sqrt{s_{\text{NN}}}$) of 13 TeV (pp) and 5.02 TeV (p-Pb). In both pp and p-Pb systems, collisions are categorized into high-multiplicity (HM) and low-multiplicity (LM) events based on the charged particles detected within the pseudorapidity ranges $2.8 < \eta < 5.1$ and $-3.7 < \eta < -1.7$, respectively. Additionally, a selection criterion on the number of reconstructed and efficiency-corrected charged particles (N_{ch}) with $0.2 < p_T < 3.0 \text{ GeV}/c$ at midrapidity ($|\eta| < 0.8$) is applied, resulting in the same average N_{ch} ($\langle N_{\text{ch}} \rangle \approx 35$) in high-multiplicity events for both p-Pb and pp collisions. The event, track selection, and particle identification are discussed in the

methods section A.

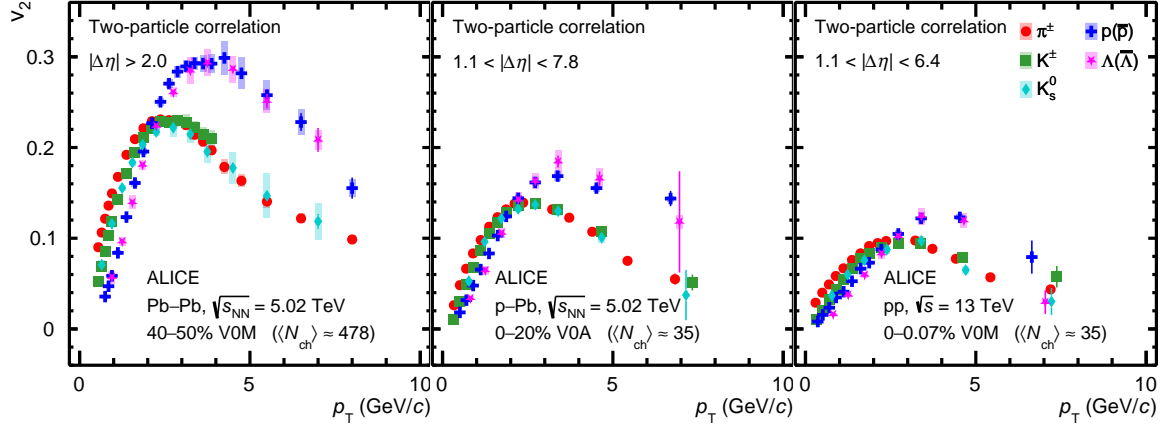


Figure 2: Left: p_T -differential v_2 measured with the two-particle correlation method [40] for mesons (π^\pm, K^\pm, K_S^0) and baryons ($p+\bar{p}, \Lambda+\bar{\Lambda}$) in semicentral Pb–Pb collisions at $\sqrt{s_{NN}} = 5.02$ TeV. Middle: p_T -differential v_2 measured with the two-particle correlation method for mesons (π^\pm, K^\pm, K_S^0) and baryons ($p+\bar{p}, \Lambda+\bar{\Lambda}$) in high-multiplicity p–Pb collisions at $\sqrt{s_{NN}} = 5.02$ TeV. Right: Same for pp collisions at $\sqrt{s} = 13$ TeV. $\langle N_{ch} \rangle$ is the average number of reconstructed, efficiency-corrected charged particles with $0.2 < p_T < 3.0$ GeV/ c at midrapidity ($|\eta| < 0.8$).

As Ψ_n used in Eq. 1 cannot be experimentally determined, the v_2 of hadrons can be obtained using two-particle azimuthal angle correlations (2PC) [21] via the three-subevent method [41]. This method employs reference particles selected in the forward and backward rapidity regions in addition to the identified hadrons selected at midrapidity, allowing a significant pseudorapidity separation between the two correlated particles, $1.1 < |\Delta\eta| < 7.8$ in p–Pb, and $1.1 < |\Delta\eta| < 6.4$ in pp collisions. The difference in the maximum available $|\Delta\eta|$ separation between pp and p–Pb collisions is due to the different performance of the forward/backward detectors in different data-taking periods. However, for each collision system, the final results are estimated with varying $|\Delta\eta|$ separations and found to be consistent with each other. This large $\Delta\eta$ separation suppresses the non-flow contamination effects due to the azimuthal angle correlations between particles produced from resonance decays and jets [42]. To further minimize the remaining non-flow effects, a template fit method [22] is employed to fit the two-particle correlation functions. The non-flow template is obtained from the analysis of LM pp and p–Pb data and is explained in detail in section A. This method reduces the non-flow contribution to the final v_2 results for identified particles to 6% for $p_T < 0.6$ GeV/ c and to less than 1% at higher p_T . These estimates are based on applying the template-fit method to a pure non-flow model using the PYTHIA 8 event generator [43].

Figure 2 presents the p_T -differential v_2 measurement for mesons (π^\pm, K^\pm, K_S^0) and baryons ($p+\bar{p}, \Lambda+\bar{\Lambda}$) in semicentral Pb–Pb [40], HM p–Pb and pp collisions. For Pb–Pb measurements, the two-particle correlation with $|\Delta\eta| > 2.0$ separation is used [40], whereas for p–Pb and pp collisions, a $|\Delta\eta| > 1.1$ separation is applied. It was tested that varying the $|\Delta\eta|$ separation does not significantly alter the results in Pb–Pb collisions [40]. Figure 2 shows a clear similarity in the characteristic features of v_2 among the three collision systems. The difference in the magnitude of v_2 among the three collision systems is consistent with previous measurements at the LHC [26]. For the low p_T region, $p_T < 2.0$ GeV/ c , a clear mass ordering of the v_2 coefficients is observed, providing significant evidence of radial flow in small collision systems. The presence of radial flow in small collision systems is also supported by particle spectra measurements [44]. Around $2.0 < p_T < 3.0$ GeV/ c , the v_2 coefficients of different particle species begin to cross. Beyond $p_T > 2.5$ GeV/ c , the v_2 coefficients of baryons ($p+\bar{p}, \Lambda+\bar{\Lambda}$) are consistent with each other within 1 standard deviation ($\sim 1\sigma$) up to 10 GeV/ c in Pb–Pb and p–Pb collisions and up to 6 GeV/ c in pp collisions. At the same time, the v_2 of mesons (π^\pm, K^\pm, K_S^0) are

compatible within $\sim 1\sigma$ at $p_T > 2(3)$ GeV/c for Pb–Pb and p–Pb (pp) collisions. Moreover, the v_2 of baryons is larger than that of mesons by $\sim 5\sigma$ at intermediate and higher p_T ($p_T > 3.0$ GeV/c) in all three collision systems. In heavy-ion collisions, such distinctive baryon-meson v_2 grouping at intermediate p_T is explained by anisotropic flow development at the quark level, followed by particle production via the quark-coalescence mechanism [14, 17, 18]. Existing measurements with identified particles in small collision systems presented either a single baryon or meson v_2 , limiting the opportunity to explore potential groupings among baryons and mesons [45, 46]. Other similar measurements have not shown a clear grouping and splitting of baryon and meson v_2 at intermediate p_T in small systems, differing from similar measurements in heavy-ion collisions [24]. This difference may arise from difficulties in accounting for non-flow effects in small systems. The results presented in Fig. 2 show, for the first time, a distinctive baryon-meson v_2 grouping (within 1σ) and splitting between them with high significance ($\sim 5\sigma$) at intermediate p_T in both p–Pb and pp collisions at the LHC, similar to that observed in heavy-ion collisions.

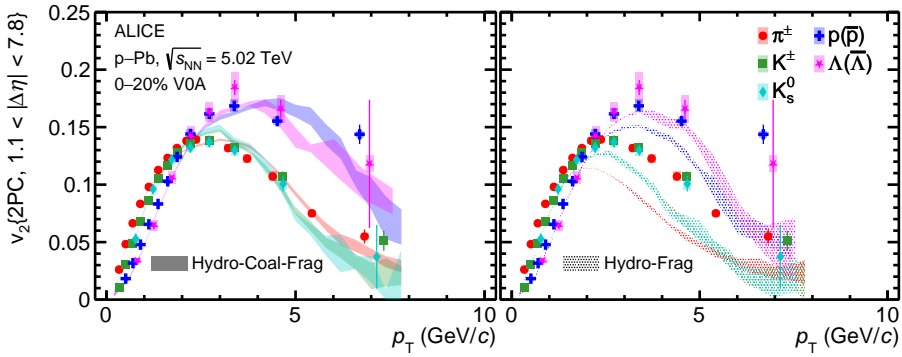


Figure 3: p_T -differential v_2 measured with two-particle correlation for mesons (π^\pm , K^\pm , K_s^0) and baryons ($p+\bar{p}$, $\Lambda+\bar{\Lambda}$) in high-multiplicity p–Pb collisions at $\sqrt{s_{NN}} = 5.02$ TeV. Comparisons with the calculations from the Hydro-Coal-Frag model (left) and the Hydro-Frag model (right) are also presented [47, 48]. Only statistical uncertainties are shown for the calculations.

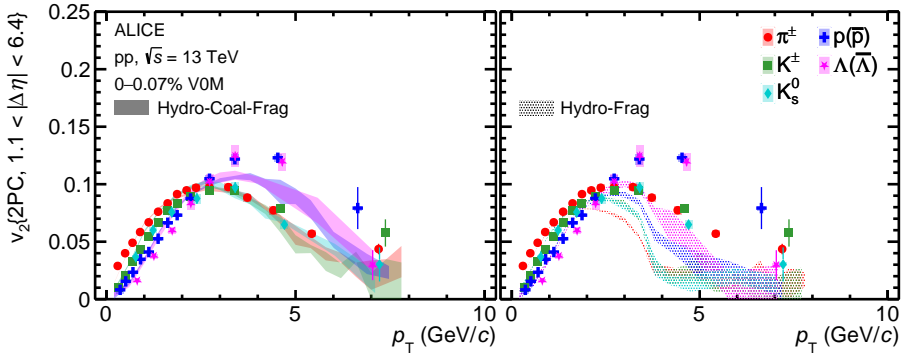


Figure 4: p_T -differential v_2 measured with two-particle correlation for mesons (π^\pm , K^\pm , K_s^0) and baryons ($p+\bar{p}$, $\Lambda+\bar{\Lambda}$) in high-multiplicity pp collisions at $\sqrt{s} = 13$ TeV. Comparisons with the calculations from the Hydro-Coal-Frag model (left) and the Hydro-Frag model (right) are also presented [47, 48]. Only statistical uncertainties are shown for the calculations.

In Figs. 3 and 4, the measurements are compared with the state-of-the-art calculations using the Hydro-Coal-Frag hybrid model [47, 48] for p–Pb and pp collisions, respectively. At low p_T , this model incorporates the hydrodynamic evolution of a quark-gluon plasma with a partonic equation of state, followed by the formation of quarks before hadronization. At high p_T , it accounts for interactions between high-energy partons and the medium using the linear Boltzmann transport (LBT) model, combined with

hadronization via quark fragmentation. The intermediate p_T hadrons are produced from the coalescence of quarks originating from both hydrodynamic evolution and jet-medium interactions. Finally, hadronic interactions occur after hadronization. This model provides a comprehensive explanation for both hadron production and anisotropic flow over a wide p_T range in high-energy heavy-ion collisions [49]. It emphasizes the crucial role of partonic flow and particle production through quark coalescence in heavy-ion collisions, where the QGP is formed. In Fig. 3, the model parameters are tuned to describe the p_T spectra of identified hadrons in high-multiplicity p–Pb collisions at $\sqrt{s_{NN}} = 5.02$ TeV [47]. The figure demonstrates that the Hydro-Coal-Frag model successfully reproduces the baryon-meson v_2 splitting and grouping features for $p_T < 8$ GeV/c as observed in the experimental data. In contrast, the calculation from the Hydro-Frag model, which does not include the quark-coalescence process, strongly underestimates the v_2 coefficients of all identified hadrons for $p_T > 4$ GeV/c. Moreover, despite parameter adjustments, the Hydro-Frag model fails to even qualitatively reproduce the baryon-meson v_2 splitting and grouping at intermediate p_T [48].

The comparison between the measurements and the model prediction for pp collisions at $\sqrt{s} = 13$ TeV is presented in Fig. 4. The model parameters are calibrated using p_T spectra of identified hadrons from a different multiplicity interval than the one used in this paper. Still, the Hydro-Coal-Frag picture can explain the mass ordering of v_2 for p_T up to 3 GeV/c combined with the crossing between v_2 of baryons and mesons at $p_T \approx 3$ GeV/c, consistent with the data. Most importantly, the baryon-meson splitting and grouping of v_2 can be qualitatively reproduced by the Hydro-Coal-Frag model up to approximately 6–7 GeV/c. In contrast, neither of these features is captured by the Hydro-Frag model. The crossing between v_2 of different particles occurs at about 2 GeV/c, and only mass ordering is observed in this calculation [48]. The ordering is reversed for $2.5 < p_T < 5$ GeV/c compared to $p_T < 2.5$ GeV/c, similar to the Hydro-Frag calculations in p–Pb collisions shown in Fig. 3. Therefore, these results provide evidence of hadronization via coalescence of flowing quarks in small collision systems at the LHC.

Other theoretical calculations that predict a flow pattern in high multiplicity events of small collision systems have also been studied. Since the presented measurements are based on long-range (i.e., large $|\Delta\eta|$ separation) two-particle correlations, they are predominantly influenced by geometry-driven effects, as the initial momentum anisotropy in the CGC approach generates only short-range correlations [36]. The hadronic rescatterings in UrQMD can mimic the long-range two-particle correlation and mass dependence of v_2 at low p_T [35], but do not generate any baryon-meson v_2 splitting and grouping. The PYTHIA 8 model, with color ropes enabled in the hadronization process, can describe the strangeness enhancement in pp collisions [27] without the formation of a QGP [50], but cannot generate long-range correlations. Interestingly, the string-string repulsion in the string-shoving version of PYTHIA 8 can generate long-range two-particle correlations [37, 51], but it produces negative flow coefficients after the template fit, in contrast to the positive flow coefficients observed in the data. In small systems, transport models like AMPT [34], which generate only a few partonic interactions during system evolution and incorporate the quark-coalescence model of hadronization, can approximately describe the v_2 at low p_T . However, they fail to even qualitatively explain the baryon-meson v_2 grouping and splitting feature observed at intermediate p_T [52]. This indicates that anisotropic flow is developed in a dense partonic system and propagated to the level of hadrons via the quark coalescence process.

In summary, the v_2 for the identified hadrons in high-multiplicity p–Pb collisions at $\sqrt{s_{NN}} = 5.02$ TeV and pp collisions at $\sqrt{s} = 13$ TeV has been presented as a function of p_T and compared with measurements in semicentral Pb–Pb collisions at $\sqrt{s_{NN}} = 5.02$ TeV. For the first time, a characteristic grouping (within $\sim 1\sigma$) and splitting (with $\sim 5\sigma$) of v_2 for mesons (π^\pm, K^\pm, K_S^0) and baryons ($p+\bar{p}, \Lambda+\bar{\Lambda}$) at intermediate p_T , similar to measurements in heavy-ion collisions, is observed in both p–Pb and pp collisions. The Hydro-Coal-Frag model, incorporating partonic flow and quark coalescence, provides the best possible description of the data to date in both heavy-ion and small collision systems. Alternative approaches fail to even qualitatively reproduce the baryon-meson v_2 splitting and grouping at interme-

ate p_T . The presented measurements and the comparisons with available theoretical model calculations provide evidence that the system created in high-multiplicity p–Pb and pp collisions includes a stage with collectively flowing partons, similar to the one observed in heavy-ion collisions.

Acknowledgments

The ALICE Collaboration would like to thank Huichao Song and Wenbin Zhao for providing the latest calculations from the state-of-the-art models.

The ALICE Collaboration would like to thank all its engineers and technicians for their invaluable contributions to the construction of the experiment and the CERN accelerator teams for the outstanding performance of the LHC complex. The ALICE Collaboration gratefully acknowledges the resources and support provided by all Grid centres and the Worldwide LHC Computing Grid (WLCG) collaboration. The ALICE Collaboration acknowledges the following funding agencies for their support in building and running the ALICE detector: A. I. Alikhanyan National Science Laboratory (Yerevan Physics Institute) Foundation (ANSL), State Committee of Science and World Federation of Scientists (WFS), Armenia; Austrian Academy of Sciences, Austrian Science Fund (FWF): [M 2467-N36] and Nationalstiftung für Forschung, Technologie und Entwicklung, Austria; Ministry of Communications and High Technologies, National Nuclear Research Center, Azerbaijan; Conselho Nacional de Desenvolvimento Científico e Tecnológico (CNPq), Financiadora de Estudos e Projetos (Finep), Fundação de Amparo à Pesquisa do Estado de São Paulo (FAPESP) and Universidade Federal do Rio Grande do Sul (UFRGS), Brazil; Bulgarian Ministry of Education and Science, within the National Roadmap for Research Infrastructures 2020-2027 (object CERN), Bulgaria; Ministry of Education of China (MOEC) , Ministry of Science & Technology of China (MSTC) and National Natural Science Foundation of China (NSFC), China; Ministry of Science and Education and Croatian Science Foundation, Croatia; Centro de Aplicaciones Tecnológicas y Desarrollo Nuclear (CEADEN), Cubaenergía, Cuba; Ministry of Education, Youth and Sports of the Czech Republic, Czech Republic; The Danish Council for Independent Research | Natural Sciences, the VILLUM FONDEN and Danish National Research Foundation (DNRF), Denmark; Helsinki Institute of Physics (HIP), Finland; Commissariat à l’Energie Atomique (CEA) and Institut National de Physique Nucléaire et de Physique des Particules (IN2P3) and Centre National de la Recherche Scientifique (CNRS), France; Bundesministerium für Bildung und Forschung (BMBF) and GSI Helmholtzzentrum für Schwerionenforschung GmbH, Germany; General Secretariat for Research and Technology, Ministry of Education, Research and Religions, Greece; National Research, Development and Innovation Office, Hungary; Department of Atomic Energy Government of India (DAE), Department of Science and Technology, Government of India (DST), University Grants Commission, Government of India (UGC) and Council of Scientific and Industrial Research (CSIR), India; National Research and Innovation Agency - BRIN, Indonesia; Istituto Nazionale di Fisica Nucleare (INFN), Italy; Japanese Ministry of Education, Culture, Sports, Science and Technology (MEXT) and Japan Society for the Promotion of Science (JSPS) KAKENHI, Japan; Consejo Nacional de Ciencia (CONACYT) y Tecnología, through Fondo de Cooperación Internacional en Ciencia y Tecnología (FONCICYT) and Dirección General de Asuntos del Personal Académico (DGAPA), Mexico; Nederlandse Organisatie voor Wetenschappelijk Onderzoek (NWO), Netherlands; The Research Council of Norway, Norway; Pontificia Universidad Católica del Perú, Peru; Ministry of Science and Higher Education, National Science Centre and WUT ID-UB, Poland; Korea Institute of Science and Technology Information and National Research Foundation of Korea (NRF), Republic of Korea; Ministry of Education and Scientific Research, Institute of Atomic Physics, Ministry of Research and Innovation and Institute of Atomic Physics and Universitatea Nationala de Stiinta si Tehnologie Politehnica Bucuresti, Romania; Ministry of Education, Science, Research and Sport of the Slovak Republic, Slovakia; National Research Foundation of South Africa, South Africa; Swedish Research Council (VR) and Knut & Alice Wallenberg Foundation (KAW), Sweden; European Organization for Nuclear Research, Switzerland; Suranaree University

of Technology (SUT), National Science and Technology Development Agency (NSTDA) and National Science, Research and Innovation Fund (NSRF via PMU-B B05F650021), Thailand; Turkish Energy, Nuclear and Mineral Research Agency (TENMAK), Turkey; National Academy of Sciences of Ukraine, Ukraine; Science and Technology Facilities Council (STFC), United Kingdom; National Science Foundation of the United States of America (NSF) and United States Department of Energy, Office of Nuclear Physics (DOE NP), United States of America. In addition, individual groups or members have received support from: Czech Science Foundation (grant no. 23-07499S), Czech Republic; FORTE project, reg. no. CZ.02.01.01/00/22_008/0004632, Czech Republic, co-funded by the European Union, Czech Republic; European Research Council (grant no. 950692), European Union; ICSC - Centro Nazionale di Ricerca in High Performance Computing, Big Data and Quantum Computing, European Union - NextGenerationEU; Academy of Finland (Center of Excellence in Quark Matter) (grant nos. 346327, 346328), Finland; Deutsche Forschungs Gemeinschaft (DFG, German Research Foundation) “Neutrinos and Dark Matter in Astro- and Particle Physics” (grant no. SFB 1258), Germany.

References

- [1] ALICE Collaboration, S. Acharya *et al.*, “The ALICE experiment: a journey through QCD”, *Eur. Phys. J. C* **84** (2024) 813, arXiv:2211.04384 [nucl-ex].
- [2] J.-Y. Ollitrault, “Anisotropy as a signature of transverse collective flow”, *Phys. Rev. D* **46** (1992) 229–245.
- [3] S. Voloshin and Y. Zhang, “Flow study in relativistic nuclear collisions by Fourier expansion of azimuthal particle distributions”, *Z. Phys. C* **70** (1996) 665–672, arXiv:hep-ph/9407282 [hep-ph].
- [4] ALICE Collaboration, K. Aamodt *et al.*, “Higher harmonic anisotropic flow measurements of charged particles in Pb–Pb collisions at $\sqrt{s_{\text{NN}}} = 2.76 \text{ TeV}$ ”, *Phys. Rev. Lett.* **107** (2011) 032301, arXiv:1105.3865 [nucl-ex].
- [5] ATLAS Collaboration, G. Aad *et al.*, “Measurement of the azimuthal anisotropy for charged particle production in $\sqrt{s_{\text{NN}}} = 2.76 \text{ TeV}$ lead-lead collisions with the ATLAS detector”, *Phys. Rev. C* **86** (2012) 014907, arXiv:1203.3087 [hep-ex].
- [6] CMS Collaboration, S. Chatrchyan *et al.*, “Measurement of higher-order harmonic azimuthal anisotropy in PbPb collisions at $\sqrt{s_{\text{NN}}} = 2.76 \text{ TeV}$ ”, *Phys. Rev. C* **89** (2014) 044906, arXiv:1310.8651 [nucl-ex].
- [7] STAR Collaboration, B. I. Abelev *et al.*, “Long range rapidity correlations and jet production in high energy nuclear collisions”, *Phys. Rev. C* **80** (2009) 064912, arXiv:0909.0191 [nucl-ex].
- [8] ALICE Collaboration, J. Adam *et al.*, “Anisotropic flow of charged particles in Pb–Pb collisions at $\sqrt{s_{\text{NN}}} = 5.02 \text{ TeV}$ ”, *Phys. Rev. Lett.* **116** (2016) 132302, arXiv:1602.01119 [nucl-ex].
- [9] ALICE Collaboration, S. Acharya *et al.*, “Anisotropic flow in Xe–Xe collisions at $\sqrt{s_{\text{NN}}} = 5.44 \text{ TeV}$ ”, *Phys. Lett. B* **784** (2018) 82–95, arXiv:1805.01832 [nucl-ex].
- [10] U. Heinz and R. Snellings, “Collective flow and viscosity in relativistic heavy-ion collisions”, *Ann. Rev. Nucl. Part. Sci.* **63** (2013) 123–151, arXiv:1301.2826 [nucl-th].
- [11] H. Song, Y. Zhou, and K. Gajdosova, “Collective flow and hydrodynamics in large and small systems at the LHC”, *Nucl. Sci. Tech.* **28** (2017) 99, arXiv:1703.00670 [nucl-th].
- [12] STAR Collaboration, C. Adler *et al.*, “Identified particle elliptic flow in Au + Au collisions at $\sqrt{s_{\text{NN}}} = 130\text{-GeV}$ ”, *Phys. Rev. Lett.* **87** (2001) 182301, arXiv:nucl-ex/0107003.

- [13] **PHENIX** Collaboration, S. S. Adler *et al.*, “Elliptic flow of identified hadrons in Au+Au collisions at $\sqrt{s_{\text{NN}}} = 200\text{-GeV}$ ”, *Phys. Rev. Lett.* **91** (2003) 182301, [arXiv:nucl-ex/0305013](#).
- [14] **ALICE** Collaboration, B. B. Abelev *et al.*, “Elliptic flow of identified hadrons in Pb–Pb collisions at $\sqrt{s_{\text{NN}}} = 2.76\text{ TeV}$ ”, *JHEP* **06** (2015) 190, [arXiv:1405.4632 \[nucl-ex\]](#).
- [15] S. A. Voloshin, “Transverse radial expansion and directed flow”, *Phys. Rev. C* **55** (1997) R1630–R1632, [arXiv:nucl-th/9611038](#).
- [16] P. Huovinen, P. F. Kolb, U. W. Heinz, P. V. Ruuskanen, and S. A. Voloshin, “Radial and elliptic flow at RHIC: Further predictions”, *Phys. Lett. B* **503** (2001) 58–64, [arXiv:hep-ph/0101136](#).
- [17] **STAR** Collaboration, J. Adams *et al.*, “Particle type dependence of azimuthal anisotropy and nuclear modification of particle production in Au + Au collisions at $\sqrt{s_{\text{NN}}} = 200\text{-GeV}$ ”, *Phys. Rev. Lett.* **92** (2004) 052302, [arXiv:nucl-ex/0306007](#).
- [18] **PHENIX** Collaboration, A. Adare *et al.*, “Scaling properties of azimuthal anisotropy in Au+Au and Cu+Cu collisions at $\sqrt{s_{\text{NN}}} = 200\text{ GeV}$ ”, *Phys. Rev. Lett.* **98** (2007) 162301, [arXiv:nucl-ex/0608033](#).
- [19] D. Molnar and S. A. Voloshin, “Elliptic flow at large transverse momenta from quark coalescence”, *Phys. Rev. Lett.* **91** (2003) 092301, [arXiv:nucl-th/0302014](#).
- [20] **CMS** Collaboration, V. Khachatryan *et al.*, “Observation of Long-Range Near-Side Angular Correlations in Proton-Proton Collisions at the LHC”, *JHEP* **09** (2010) 091, [arXiv:1009.4122 \[hep-ex\]](#).
- [21] **ALICE** Collaboration, B. B. Abelev *et al.*, “Long-range angular correlations of π , K and p in p–Pb collisions at $\sqrt{s_{\text{NN}}} = 5.02\text{ TeV}$ ”, *Phys. Lett. B* **726** (2013) 164–177, [arXiv:1307.3237 \[nucl-ex\]](#).
- [22] **ATLAS** Collaboration, G. Aad *et al.*, “Observation of Long-Range Elliptic Azimuthal Anisotropies in $\sqrt{s} = 13$ and 2.76 TeV pp Collisions with the ATLAS Detector”, *Phys. Rev. Lett.* **116** (2016) 172301, [arXiv:1509.04776 \[hep-ex\]](#).
- [23] **PHENIX** Collaboration, C. Aidala *et al.*, “Creation of quark–gluon plasma droplets with three distinct geometries”, *Nature Phys.* **15** (2019) 214–220, [arXiv:1805.02973 \[nucl-ex\]](#).
- [24] **CMS** Collaboration, A. M. Sirunyan *et al.*, “Elliptic flow of charm and strange hadrons in high-multiplicity pPb collisions at $\sqrt{s_{\text{NN}}} = 8.16\text{ TeV}$ ”, *Phys. Rev. Lett.* **121** (2018) 082301, [arXiv:1804.09767 \[hep-ex\]](#).
- [25] **CMS** Collaboration, V. Khachatryan *et al.*, “Long-range two-particle correlations of strange hadrons with charged particles in pPb and PbPb collisions at LHC energies”, *Phys. Lett. B* **742** (2015) 200–224, [arXiv:1409.3392 \[nucl-ex\]](#).
- [26] **ALICE** Collaboration, S. Acharya *et al.*, “Investigations of Anisotropic Flow Using Multiparticle Azimuthal Correlations in pp, p–Pb, Xe–Xe, and Pb–Pb Collisions at the LHC”, *Phys. Rev. Lett.* **123** (2019) 142301, [arXiv:1903.01790 \[nucl-ex\]](#).
- [27] **ALICE** Collaboration, J. Adam *et al.*, “Enhanced production of multi-strange hadrons in high-multiplicity proton-proton collisions”, *Nature Phys.* **13** (2017) 535–539, [arXiv:1606.07424 \[nucl-ex\]](#).

- [28] K. Dusling, M. Mace, and R. Venugopalan, “Multiparticle collectivity from initial state correlations in high energy proton-nucleus collisions”, *Phys. Rev. Lett.* **120** (2018) 042002, arXiv:1705.00745 [hep-ph].
- [29] P. Bozek, “Collective flow in p–Pb and d–Pb collisions at TeV energies”, *Phys. Rev. C* **85** (2012) 014911, arXiv:1112.0915 [hep-ph].
- [30] H. Mäntysaari, B. Schenke, C. Shen, and P. Tribedy, “Imprints of fluctuating proton shapes on flow in proton-lead collisions at the LHC”, *Phys. Lett. B* **772** (2017) 681–686, arXiv:1705.03177 [nucl-th].
- [31] R. D. Weller and P. Romatschke, “One fluid to rule them all: viscous hydrodynamic description of event-by-event central p+p, p+Pb and Pb+Pb collisions at $\sqrt{s} = 5.02$ TeV”, *Phys. Lett. B* **774** (2017) 351–356, arXiv:1701.07145 [nucl-th].
- [32] W. Zhao, Y. Zhou, H. Xu, W. Deng, and H. Song, “Hydrodynamic collectivity in proton–proton collisions at 13 TeV”, *Phys. Lett. B* **780** (2018) 495–500, arXiv:1801.00271 [nucl-th].
- [33] A. Kurkela, U. A. Wiedemann, and B. Wu, “Nearly isentropic flow at sizeable η/s ”, *Phys. Lett. B* **783** (2018) 274–279, arXiv:1803.02072 [hep-ph].
- [34] L. He, T. Edmonds, Z.-W. Lin, F. Liu, D. Molnar, and F. Wang, “Anisotropic parton escape is the dominant source of azimuthal anisotropy in transport models”, *Phys. Lett. B* **753** (2016) 506–510, arXiv:1502.05572 [nucl-th].
- [35] Y. Zhou, X. Zhu, P. Li, and H. Song, “Investigation of possible hadronic flow in $\sqrt{s_{\text{NN}}} = 5.02$ TeV p–Pb collisions”, *Phys. Rev. C* **91** (2015) 064908, arXiv:1503.06986 [nucl-th].
- [36] B. Schenke, S. Schlichting, and P. Singh, “Rapidity dependence of initial state geometry and momentum correlations in p+Pb collisions”, *Phys. Rev. D* **105** (2022) 094023, arXiv:2201.08864 [nucl-th].
- [37] C. Bierlich, G. Gustafson, and L. Lönnblad, “Collectivity without plasma in hadronic collisions”, *Phys. Lett. B* **779** (2018) 58–63, arXiv:1710.09725 [hep-ph].
- [38] ALICE Collaboration, K. Aamodt *et al.*, “The ALICE experiment at the CERN LHC”, *JINST* **3** (2008) S08002.
- [39] ALICE Collaboration, B. B. Abelev *et al.*, “Performance of the ALICE Experiment at the CERN LHC”, *Int. J. Mod. Phys. A* **29** (2014) 1430044, arXiv:1402.4476 [nucl-ex].
- [40] ALICE Collaboration, S. Acharya *et al.*, “Anisotropic flow of identified particles in Pb–Pb collisions at $\sqrt{s_{\text{NN}}} = 5.02$ TeV”, *JHEP* **09** (2018) 006, arXiv:1805.04390 [nucl-ex].
- [41] ALICE Collaboration, S. Acharya *et al.*, “Azimuthal anisotropy of jet particles in p-Pb and Pb-Pb collisions at $\sqrt{s_{\text{NN}}} = 5.02$ TeV”, *JHEP* **08** (2024) 234, arXiv:2212.12609 [nucl-ex].
- [42] ALICE Collaboration, S. Acharya *et al.*, “Measurement of inclusive charged-particle jet production in pp and p-Pb collisions at $\sqrt{s_{\text{NN}}} = 5.02$ TeV”, *JHEP* **05** (2024) 041, arXiv:2307.10860 [nucl-ex].
- [43] C. Bierlich *et al.*, “A comprehensive guide to the physics and usage of PYTHIA 8.3”, *SciPost Phys. Codeb.* **2022** (2022) 8, arXiv:2203.11601 [hep-ph].
- [44] ALICE Collaboration, B. B. Abelev *et al.*, “Multiplicity Dependence of Pion, Kaon, Proton and Lambda Production in p-Pb Collisions at $\sqrt{s_{\text{NN}}} = 5.02$ TeV”, *Phys. Lett. B* **728** (2014) 25–38, arXiv:1307.6796 [nucl-ex].

- [45] CMS Collaboration, V. Khachatryan *et al.*, “Evidence for collectivity in pp collisions at the LHC”, *Phys. Lett. B* **765** (2017) 193–220, arXiv:1606.06198 [nucl-ex].
- [46] CMS Collaboration, A. M. Sirunyan *et al.*, “Observation of prompt J/ ψ meson elliptic flow in high-multiplicity pPb collisions at $\sqrt{s_{NN}} = 8.16$ TeV”, *Phys. Lett. B* **791** (2019) 172–194, arXiv:1810.01473 [hep-ex].
- [47] W. Zhao, C. M. Ko, Y.-X. Liu, G.-Y. Qin, and H. Song, “Probing the Partonic Degrees of Freedom in High-Multiplicity p-Pb collisions at $\sqrt{s_{NN}} = 5.02$ TeV”, *Phys. Rev. Lett.* **125** (2020) 072301, arXiv:1911.00826 [nucl-th].
- [48] Y. Wang, W. Zhao, and H. Song, “Exploring the partonic collectivity in small systems at the LHC”, arXiv:2401.00913 [nucl-th].
- [49] W. Zhao, W. Ke, W. Chen, T. Luo, and X.-N. Wang, “From Hydrodynamics to Jet Quenching, Coalescence, and Hadron Cascade: A Coupled Approach to Solving the RAA \otimes v2 Puzzle”, *Phys. Rev. Lett.* **128** (2022) 022302, arXiv:2103.14657 [hep-ph].
- [50] C. Bierlich, S. Chakraborty, G. Gustafson, and L. Lönnblad, “Strangeness enhancement across collision systems without a plasma”, *Phys. Lett. B* **835** (2022) 137571, arXiv:2205.11170 [hep-ph].
- [51] C. Bierlich, G. Gustafson, L. Lönnblad, and A. Tarasov, “Effects of Overlapping Strings in pp Collisions”, *JHEP* **03** (2015) 148, arXiv:1412.6259 [hep-ph].
- [52] S.-Y. Tang, L. Zheng, X.-M. Zhang, and R.-Z. Wan, “Investigating the elliptic anisotropy of identified particles in p-Pb collisions with a multi-phase transport model”, *Nucl. Sci. Tech.* **35** (2024) 32, arXiv:2303.06577 [hep-ph].
- [53] ALICE Collaboration, “ALICE 2016-2017-2018 luminosity determination for pp collisions at $\sqrt{s} = 13$ TeV”, <https://cds.cern.ch/record/2776672>.
- [54] ALICE Collaboration, B. B. Abelev *et al.*, “Measurement of visible cross sections in proton-lead collisions at $\sqrt{s_{NN}} = 5.02$ TeV in van der Meer scans with the ALICE detector”, *JINST* **9** (2014) P11003, arXiv:1405.1849 [nucl-ex].
- [55] Particle Data Group Collaboration, S. Navas *et al.*, “Review of particle physics”, *Phys. Rev. D* **110** (2024) 030001.
- [56] R. Barlow, “Systematic errors: Facts and fictions”, in *Conference on Advanced Statistical Techniques in Particle Physics*, pp. 134–144. 7, 2002. arXiv:hep-ex/0207026.

A Methods

A.1 Event selection

The analyzed data samples are from pp collisions at $\sqrt{s} = 13$ TeV and p–Pb collisions at $\sqrt{s_{\text{NN}}} = 5.02$ TeV, collected by the ALICE detector during the LHC Run 2 data-taking campaign between 2016 and 2018. An extensive description of all subdetectors of ALICE can be found in Refs. [38, 39]. The collected data are classified based on the specific triggering conditions. Minimum bias (MB) events for both pp and p–Pb collisions are triggered using a coincidence signal in the two scintillator arrays of the V0 detector, which cover the pseudorapidity ranges $2.8 < \eta < 5.1$ (V0A) and $-3.7 < \eta < -1.7$ (V0C), respectively. To avoid the possibility of overlap between HM and LM event classes, additional requirements on the number of reconstructed and efficiency-corrected charged particles (N_{ch}) within the acceptance of $|\eta| < 0.8$ and transverse momentum $0.2 < p_{\text{T}} < 3$ GeV/c are introduced. For p–Pb collisions, the collisions of the 0–20% and 60–100% V0A-centrality are used as the HM and LM events, with an additional criterion of $N_{\text{ch}} < 20$ applied to the LM sample. In pp collisions, HM events are selected from the 0.07% of events with the highest multiplicity. This selection uses a special HM trigger based on the amplitude of the V0M detector arrays (V0A + V0C) and requires $N_{\text{ch}} > 25$. For the LM event class, MB events with $N_{\text{ch}} < 20$ are selected. Only events with a reconstructed primary vertex (PV) within ± 10 cm from the nominal interaction point along the beam line are selected. Background events due to interaction between the beam and the residual gas molecules in the beam pipe are removed using the information from the Silicon Pixel Detector (SPD) and V0 detectors. The out-of-bunch pileup events are rejected using a correlation between the multiplicities in the V0 and Forward-Multiplicity-Detector (FMD) [38]. The in-bunch pileup is reduced by rejecting events with multiple vertices. The event selections result in a sample of 226×10^6 HM and 572×10^6 LM pp collisions, corresponding to integrated luminosities of approximately 4 nb^{-1} and 10 nb^{-1} , respectively [53]. For p–Pb, the analyzed data sample consists of 101×10^6 HM collisions and 198×10^6 LM collisions, corresponding to integrated luminosities of about 0.05 nb^{-1} and 0.09 nb^{-1} , respectively [54]. In this analysis, the HM events are used for the flow measurements, whereas the LM events are used for the baseline non-flow estimation.

A.2 Track reconstruction

The charged particles at midrapidity are reconstructed using the Inner Tracking System (ITS) and the Time Projection Chamber (TPC). The selected tracks have at least 70 TPC space points (out of a maximum of 159) fitted for track reconstruction with χ^2 per degree of freedom lower than four. The reconstructed tracks from the TPC and the ITS must coincide to ensure the consistency of the reconstruction method. Additionally, a minimum of two hits are required in the ITS to improve the momentum resolution. The pseudorapidity of the selected tracks is required to be within $|\eta| < 0.8$ to reject tracks with reduced reconstruction efficiency at the detector edges. To reduce the contamination from secondary particles, the distance-of-closest approach (DCA) of the selected tracks to the PV must be within 2 cm in the longitudinal direction. Furthermore, a p_{T} -dependent DCA selection in the transverse plane, ranging from 0.2 cm at $p_{\text{T}} = 0.2$ GeV/c to 0.02 cm at $p_{\text{T}} = 5.0$ GeV/c, is applied. This criterion suppresses the residual contamination from secondary particles from weak decays and interactions in the detector material. The reference particles used for the construction of long-range di-hadron correlation functions are selected from the FMD detector segments located at forward (FMD1,2 with $1.7 < \eta < 5.1$) and backward (FMD3 with $-3.1 < \eta < -1.7$) rapidity regions.

A.3 Particle identification and reconstruction

The charged tracks are identified as π^\pm , K^\pm , and $p+\bar{p}$ based on the specific energy loss (dE/dx) information in the TPC and the velocity information from the Time-of-Flight (TOF) detector. A Bayesian approach [40] is used to identify particle species at a given p_{T} using the correlation of the normalized differences between the measured and the expected signal in the TPC ($n\sigma_{\text{TPC}}$) and the TOF ($n\sigma_{\text{TOF}}$),

respectively. In this method, the signals are converted into probabilities and folded with the expected abundances (priors) of each particle species. To ensure high purity of the selected sample, a minimal probability threshold of 0.95 for π^\pm and 0.85 for K^\pm and $p+\bar{p}$ is set. In addition, the tracks with proper TOF information are required to be within $|n\sigma_{\text{TPC}}| < 3$ and $|n\sigma_{\text{TOF}}| < 3$. The resulting purity, estimated using Monte Carlo (MC) simulations, is higher than 95% for π^\pm for $0.2 < p_T < 10 \text{ GeV}/c$, above 80% for K^\pm for $0.3 < p_T < 10 \text{ GeV}/c$, and reaches values larger than 90% for $p+\bar{p}$ for $0.5 < p_T < 10 \text{ GeV}/c$. The high purity of the studied sample reduces the uncertainties due to particle misidentification. The K_S^0 and $\Lambda+\bar{\Lambda}$ are weakly decaying neutral particles, reconstructed by calculating the invariant mass of the daughter particles from the most probable decay channels of $K_S^0 \rightarrow \pi^+ + \pi^-$ and $\Lambda \rightarrow p + \pi^-$ ($\bar{\Lambda} \rightarrow \bar{p} + \pi^+$) with branching ratios of 69.2%($\pm 0.05\%$) and 64.1%($\pm 0.5\%$) [55], respectively. The combinatorial background is suppressed by using a set of selection criteria on the decay topology used in the previous K_S^0 and Λ measurements in ALICE [27]. The K_S^0 and $\Lambda+\bar{\Lambda}$ candidates are selected within the rapidity range $|y| < 0.5$ inside the TPC, and the daughter tracks are used to reconstruct the secondary decay vertex (SV) in the offline reconstruction. The SV is required to be more than 0.5 cm away from the PV, and the reconstructed proper lifetime, defined as mL/p , (m being the particle mass, L the distance between the primary and secondary vertices, and p the particle momentum) should be smaller than 20 cm and 30 cm for K_S^0 and Λ ($\bar{\Lambda}$) candidates, respectively. The oppositely charged daughter tracks are combined only if they are identified as pions or protons based on the TPC dE/dx hypothesis ($< 3\sigma$). A set of topological cuts, such as the distance of closest approach (DCA) of the daughter tracks to the primary vertex (> 0.06 cm), DCA between the daughter tracks (< 1 cm), and cosine of the pointing angle, which is the angle between the momentum direction of the mother particle and the direction from the PV to the decay point (> 0.97 for K_S^0 and > 0.995 for $\Lambda(\bar{\Lambda})$) are applied to reduce the combinatorial background contribution to the invariant mass spectrum.

A.4 Correlation function and template fit method

The correlation function is obtained among two sets of particles classified as trigger and associated. Trigger particles are used as a reference, and the angular distribution of associated particles is measured relative to the trigger particles [21]. In this analysis, the 2D correlation function is constructed as a function of the difference in azimuthal angle $\Delta\varphi = \varphi_{\text{trigger}} - \varphi_{\text{associated}}$ and pseudorapidity $\Delta\eta = \eta_{\text{trigger}} - \eta_{\text{associated}}$ with trigger and associated particles from different detectors. Three sets of correlation functions are constructed to estimate the v_2 of identified particles (π^\pm , K^\pm , $p+\bar{p}$, K_S^0 , and $\Lambda+\bar{\Lambda}$). The identified particles in the TPC are correlated with unidentified reference particles reconstructed within the FMD acceptance in positive (FMD1,2) and negative (FMD3) rapidity regions to construct two sets (TPC–FMD1,2 and TPC–FMD3) of correlation functions. The third correlation function is constructed using two reference particles from the FMD1,2 and FMD3 detector segments. The pair acceptance effect due to the finite size of the detectors is corrected by dividing the same-event correlation functions with mixed-event correlation functions. The mixed-event correlation function is constructed by correlating the trigger particles in one event with the associated particles from other events belonging to the same multiplicity event class and with PV within a given 2cm wide interval. The mixed event is normalized using a constant estimated by averaging over all $\Delta\varphi$ bins at the $\Delta\eta$ value where the mixed event correlation function reaches its maximum. The corrected correlation function is obtained as a ratio of the same and mixed event correlation function for each PV position. The final correlation function for an event class (HM or LM events) is calculated after averaging the correlation functions over all PV positions. For each of the 2D correlation functions (TPC–FMD1,2, TPC–FMD3, and FMD1,2–FMD3), the projection along the $\Delta\varphi$ axis is calculated for both HM and LM cases. The $\Delta\varphi$ projections from LM collisions serve as a template for subsequent fitting of the $\Delta\varphi$ projections from HM collisions to extract the v_2 coefficients using the template fit method. The template fit method assumes that high-multiplicity (HM) collisions are a superposition of low-multiplicity (LM) collisions, which primarily contain non-flow effects with

some residual flow, along with an additional flow modulation, i.e.,

$$Y(\Delta\varphi)^{\text{HM}} = FY(\Delta\varphi)^{\text{LM}} + G \left[1 + \sum_{n=2}^{\infty} 2V_{n\Delta} \cos(n\Delta\varphi) \right], \quad (\text{A.1})$$

where $Y(\Delta\varphi)^{\text{HM}}$ and $Y(\Delta\varphi)^{\text{LM}}$ are the one dimensional $\Delta\varphi$ projections of the 2D correlation functions obtained in HM and LM collisions with F and G being the scaling factors. The $V_{n\Delta}$ coefficients are estimated by fitting the correlation function with the equation A.1. The scaling factors F and G are free parameters in this template fit procedure. The final v_2 of the identified particles in the TPC is calculated by combining the $V_{2\Delta}$ estimated from the TPC–FMD1,2, TPC–FMD3, and FMD1,2–FMD3 correlation functions

$$v_2^{\text{PID}}(p_T) = \sqrt{\frac{V_{2\Delta}^{\text{TPC–FMD1,2}} V_{2\Delta}^{\text{TPC–FMD3}}}{V_{2\Delta}^{\text{FMD1,2–FMD3}}}}. \quad (\text{A.2})$$

A.5 Systematic uncertainty

The systematic uncertainties are evaluated by varying the event, track, and PID selection criteria with respect to the default ones, one at a time. For each variation, the difference between the default and varied result is estimated using the Barlow criterion [56], and a difference higher than 1σ is considered as a possible source of systematic uncertainty in the measurement. The Barlow difference is calculated for each particle species and for each p_T interval for which the final $v_2\{2\text{PC}\}$ results are presented in this paper. The Barlow ratio is calculated as

$$B = \frac{|v_2^{\text{default}} - v_2^{\text{syst}}|}{\sqrt{|\sigma_{\text{default}}^2 - \sigma_{\text{syst}}^2|}}. \quad (\text{A.3})$$

If the Barlow difference is higher than 1σ for more than $1/3$ of the total p_T intervals for any species, the contribution of that particular systematic source is included in the uncertainty of the final result. Otherwise, the contribution from that systematic source is considered negligible and does not contribute to the final systematic uncertainty. The minimum and maximum values of the relative systematic uncertainties from individual sources are presented in Tabs. A.1 and A.2 for p–Pb and pp collisions, respectively. The systematic sources listed in the tables from top to bottom include different PV intervals used for event selection, correlation between multiplicity from V0 and FMD detectors to reduce contamination in the FMD, track selection criteria, and particle identification criteria affecting the purity of the π^\pm , K^\pm and $p+\bar{p}$ samples. Other factors are topological reconstruction criteria, invariant mass reconstruction and fitting requirements impacting the signal-to-background ratios for K_S^0 and $\Lambda+\bar{\Lambda}$ candidates, the definition of the low-multiplicity template used for non-flow removal, and the estimation of residual secondary contamination in the FMD. The latter is done using a Monte Carlo event generator, by transporting the generated particles through GEANT3-simulated detector response and performing track reconstruction in the ALICE framework. The contributions from the different sources are added in quadrature to estimate the total systematic uncertainty.

Table A.1: The minimum and maximum values of the relative systematic uncertainties from individual sources for π^\pm , K^\pm , $p+\bar{p}$, K_S^0 , and $\Lambda+\bar{\Lambda}$ in p–Pb collisions. Percentage ranges are given to account for variations with p_T . The fields marked as “negl.” (negligible) denote that the uncertainties have been tested but are not statistically significant.

Uncertainty source	$v_2\{2PC, 1.1 < \Delta\eta < 7.8\}$				
	π^\pm	K^\pm	$p+\bar{p}$	K_S^0	$\Lambda+\bar{\Lambda}$
Primary vertex position	1–2%	1–3%	1–2%	negl.	negl.
FMD–V0 correlation	0–4%	0–2%	0–2%	1–4%	2–4%
Primary track quality	negl.	negl.	negl.	–	–
Bayesian threshold	negl.	negl.	negl.	–	–
Topological criteria	–	–	–	1–2%	1–4%
Invariant mass acceptance	–	–	–	negl.	3–4%
Invariant mass fit	–	–	–	negl.	1–3%
Template variation	negl.	negl.	1–2%	negl.	negl.
Secondary contamination	1%	1%	1%	1%	1%
Total	2–4%	2–3%	1–3%	2–5%	5–7%

Table A.2: The minimum and maximum values of the relative systematic uncertainties from individual sources for π^\pm , K^\pm , $p+\bar{p}$, K_S^0 , and $\Lambda+\bar{\Lambda}$ in pp collisions. Percentage ranges are given to account for variations with p_T . The fields marked as “negl.” (negligible) denote that the uncertainties have been tested but are not statistically significant.

Uncertainty source	$v_2\{2PC, 1.1 < \Delta\eta < 6.4\}$				
	π^\pm	K^\pm	$p+\bar{p}$	K_S^0	$\Lambda+\bar{\Lambda}$
Primary vertex position	0–1%	negl.	negl.	2–3%	1–3%
FMD–V0 correlation	1–2%	negl.	0–2%	1–4%	1–3%
Primary track quality	0–2%	negl.	negl.	–	–
Bayesian threshold	negl.%	0–2%	negl.	–	–
Topological criteria	–	–	–	2–4%	1–5%
Invariant mass acceptance	–	–	–	negl.	1–3%
Invariant mass fit	–	–	–	1–2%	3–4%
Template variation	0–4%	0–2%	1–3%	1–3%	2–4%
Secondary contamination	1%	1%	1%	1%	1%
Total	2–5%	2%	2–4%	4–6%	4–8%

B The ALICE Collaboration

- S. Acharya ¹²⁶, A. Agarwal¹³⁴, G. Aglieri Rinella ³², L. Aglietta ²⁴, M. Agnello ²⁹, N. Agrawal ²⁵, Z. Ahammed ¹³⁴, S. Ahmad ¹⁵, S.U. Ahn ⁷¹, I. Ahuja ³⁶, A. Akindinov ¹⁴⁰, V. Akishina³⁸, M. Al-Turany ⁹⁶, D. Aleksandrov ¹⁴⁰, B. Alessandro ⁵⁶, H.M. Alfanda ⁶, R. Alfaro Molina ⁶⁷, B. Ali ¹⁵, A. Alici ²⁵, N. Alizadehvandchali ¹¹⁵, A. Alkin ¹⁰³, J. Alme ²⁰, G. Alocco ^{24,52}, T. Alt ⁶⁴, A.R. Altamura ⁵⁰, I. Altsybeev ⁹⁴, J.R. Alvarado ⁴⁴, C.O.R. Alvarez ⁴⁴, M.N. Anaam ⁶, C. Andrei ⁴⁵, N. Andreou ¹¹⁴, A. Andronic ¹²⁵, E. Andronov ¹⁴⁰, V. Anguelov ⁹³, F. Antinori ⁵⁴, P. Antonioli ⁵¹, N. Apadula ⁷³, L. Aphecetche ¹⁰², H. Appelshäuser ⁶⁴, C. Arata ⁷², S. Arcelli ²⁵, R. Arnaldi ⁵⁶, J.G.M.C.A. Arneiro ¹⁰⁹, I.C. Arsene ¹⁹, M. Arslanbekov ¹³⁷, A. Augustinus ³², R. Averbeck ⁹⁶, D. Averyanov ¹⁴⁰, M.D. Azmi ¹⁵, H. Baba¹²³, A. Badalà ⁵³, J. Bae ¹⁰³, Y. Bae ¹⁰³, Y.W. Baek ⁴⁰, X. Bai ¹¹⁹, R. Bailhache ⁶⁴, Y. Bailung ⁴⁸, R. Bala ⁹⁰, A. Balbino ²⁹, A. Baldissari ¹²⁹, B. Balis ², Z. Banoo ⁹⁰, V. Barbasova³⁶, F. Barile ³¹, L. Barioglio ⁵⁶, M. Barlou⁷⁷, B. Barman⁴¹, G.G. Barnaföldi ⁴⁶, L.S. Barnby ¹¹⁴, E. Barreau ¹⁰², V. Barret ¹²⁶, L. Barreto ¹⁰⁹, C. Bartels ¹¹⁸, K. Barth ³², E. Bartsch ⁶⁴, N. Bastid ¹²⁶, S. Basu ⁷⁴, G. Batigne ¹⁰², D. Battistini ⁹⁴, B. Batyunya ¹⁴¹, D. Bauri⁴⁷, J.L. Bazo Alba ¹⁰⁰, I.G. Bearden ⁸², C. Beattie ¹³⁷, P. Becht ⁹⁶, D. Behera ⁴⁸, I. Belikov ¹²⁸, A.D.C. Bell Hechavarria ¹²⁵, F. Bellini ²⁵, R. Bellwied ¹¹⁵, S. Belokurova ¹⁴⁰, L.G.E. Beltran ¹⁰⁸, Y.A.V. Beltran ⁴⁴, G. Bencedi ⁴⁶, A. Bensaoula¹¹⁵, S. Beole ²⁴, Y. Berdnikov ¹⁴⁰, A. Berdnikova ⁹³, L. Bergmann ⁹³, M.G. Besoiu ⁶³, L. Betev ³², P.P. Bhaduri ¹³⁴, A. Bhasin ⁹⁰, B. Bhattacharjee ⁴¹, L. Bianchi ²⁴, J. Bielčík ³⁴, J. Bielčíková ⁸⁵, A.P. Bigot ¹²⁸, A. Bilandzic ⁹⁴, G. Biro ⁴⁶, S. Biswas ⁴, N. Bize ¹⁰², J.T. Blair ¹⁰⁷, D. Blau ¹⁴⁰, M.B. Blidaru ⁹⁶, N. Bluhme³⁸, C. Blume ⁶⁴, F. Bock ⁸⁶, T. Bodova ²⁰, J. Bok ¹⁶, L. Boldizsár ⁴⁶, M. Bombara ³⁶, P.M. Bond ³², G. Bonomi ^{133,55}, H. Borel ¹²⁹, A. Borissov ¹⁴⁰, A.G. Borquez Carcamo ⁹³, E. Botta ²⁴, Y.E.M. Bouziani ⁶⁴, L. Bratrud ⁶⁴, P. Braun-Munzinger ⁹⁶, M. Bregant ¹⁰⁹, M. Broz ³⁴, G.E. Bruno ^{95,31}, V.D. Buchakchiev ³⁵, M.D. Buckland ⁸⁴, D. Budnikov ¹⁴⁰, H. Buesching ⁶⁴, S. Bufalino ²⁹, P. Buhler ¹⁰¹, N. Burmasov ¹⁴⁰, Z. Buthelezi ^{68,122}, A. Bylinkin ²⁰, S.A. Bysiak¹⁰⁶, J.C. Cabanillas Noris ¹⁰⁸, M.F.T. Cabrera¹¹⁵, H. Caines ¹³⁷, A. Caliva ²⁸, E. Calvo Villar ¹⁰⁰, J.M.M. Camacho ¹⁰⁸, P. Camerini ²³, F.D.M. Canedo ¹⁰⁹, S.L. Cantway ¹³⁷, M. Carabas ¹¹², A.A. Carballo ³², F. Carnesecchi ³², R. Caron ¹²⁷, L.A.D. Carvalho ¹⁰⁹, J. Castillo Castellanos ¹²⁹, M. Castoldi ³², F. Catalano ³², S. Cattaruzzi ²³, R. Cerri ²⁴, I. Chakaberia ⁷³, P. Chakraborty ¹³⁵, S. Chandra ¹³⁴, S. Chapelard ³², M. Chartier ¹¹⁸, S. Chattopadhyay¹³⁴, M. Chen³⁹, T. Cheng ⁶, C. Cheshkov ¹²⁷, D. Chiappara ²⁷, V. Chibante Barroso ³², D.D. Chinellato ¹⁰¹, E.S. Chizzali ^{II,94}, J. Cho ⁵⁸, S. Cho ⁵⁸, P. Chochula ³², Z.A. Chochulska¹³⁵, D. Choudhury⁴¹, S. Choudhury⁹⁸, P. Christakoglou ⁸³, C.H. Christensen ⁸², P. Christiansen ⁷⁴, T. Chujo ¹²⁴, M. Ciacco ²⁹, C. Cicalo ⁵², F. Cindolo ⁵¹, M.R. Ciupek⁹⁶, G. Clai^{III,51}, F. Colamarria ⁵⁰, J.S. Colburn⁹⁹, D. Colella ³¹, A. Colelli³¹, M. Colocci ²⁵, M. Concas ³², G. Conesa Balbastre ⁷², Z. Conesa del Valle ¹³⁰, G. Contin ²³, J.G. Contreras ³⁴, M.L. Coquet ¹⁰², P. Cortese ^{132,56}, M.R. Cosentino ¹¹¹, F. Costa ³², S. Costanza ^{21,55}, C. Cot ¹³⁰, P. Crochet ¹²⁶, M.M. Czarnynoga¹³⁵, A. Dainese ⁵⁴, G. Dange³⁸, M.C. Danisch ⁹³, A. Danu ⁶³, P. Das ^{32,79}, S. Das ⁴, A.R. Dash ¹²⁵, S. Dash ⁴⁷, A. De Caro ²⁸, G. de Cataldo ⁵⁰, J. de Cuveland³⁸, A. De Falco ²², D. De Gruttola ²⁸, N. De Marco ⁵⁶, C. De Martin ²³, S. De Pasquale ²⁸, R. Deb ¹³³, R. Del Grande ⁹⁴, L. Dello Stritto ³², W. Deng ⁶, K.C. Devereaux¹⁸, G.G.A. de Souza¹⁰⁹, P. Dhankher ¹⁸, D. Di Bari ³¹, A. Di Mauro ³², B. Di Ruzza ¹³¹, B. Diab ¹²⁹, R.A. Diaz ^{141,7}, Y. Ding ⁶, J. Ditzel ⁶⁴, R. Divià ³², Ø. Djupsland²⁰, U. Dmitrieva ¹⁴⁰, A. Dobrin ⁶³, B. Dönigus ⁶⁴, J.M. Dubinski ¹³⁵, A. Dubla ⁹⁶, P. Dupieux ¹²⁶, N. Dzialiova¹³, T.M. Eder ¹²⁵, R.J. Ehlers ⁷³, F. Eisenhut ⁶⁴, R. Ejima ⁹¹, D. Elia ⁵⁰, B. Erazmus ¹⁰², F. Ercolelli ²⁵, B. Espagnon ¹³⁰, G. Eulisse ³², D. Evans ⁹⁹, S. Evdokimov ¹⁴⁰, L. Fabbietti ⁹⁴, M. Faggin ²³, J. Faivre ⁷², F. Fan ⁶, W. Fan ⁷³, A. Fantoni ⁴⁹, M. Fasel ⁸⁶, G. Feofilov ¹⁴⁰, A. Fernández Téllez ⁴⁴, L. Ferrandi ¹⁰⁹, M.B. Ferrer ³², A. Ferrero ¹²⁹, C. Ferrero ^{IV,56}, A. Ferretti ²⁴, V.J.G. Feuillard ⁹³, V. Filova ³⁴, D. Finogeev ¹⁴⁰, F.M. Fionda ⁵², E. Flatland³², F. Flor ^{137,115}, A.N. Flores ¹⁰⁷, S. Foertsch ⁶⁸, I. Fokin ⁹³, S. Fokin ¹⁴⁰, U. Follo ^{IV,56}, E. Fragiocomo ⁵⁷, E. Frajna ⁴⁶, U. Fuchs ³², N. Funicello ²⁸, C. Furget ⁷², A. Furs ¹⁴⁰, T. Fusayasu ⁹⁷, J.J. Gaardhøje ⁸², M. Gagliardi ²⁴, A.M. Gago ¹⁰⁰, T. Gahlaut⁴⁷, C.D. Galvan ¹⁰⁸, S. Gami⁷⁹, D.R. Gangadharan ¹¹⁵, P. Ganoti ⁷⁷, C. Garabatos ⁹⁶, J.M. Garcia ⁴⁴, T. García Chávez ⁴⁴, E. Garcia-Solis ⁹, C. Gargiulo ³², P. Gasik ⁹⁶, H.M. Gaur³⁸, A. Gautam ¹¹⁷, M.B. Gay Ducati ⁶⁶, M. Germain ¹⁰², R.A. Gernhaeuser⁹⁴, C. Ghosh¹³⁴, M. Giacalone ⁵¹, G. Gioachin ²⁹, S.K. Giri¹³⁴, P. Giubellino ^{96,56}, P. Giubilato ²⁷, A.M.C. Glaenzer ¹²⁹, P. Glässel ⁹³, E. Glimos ¹²¹, D.J.Q. Goh⁷⁵, V. Gonzalez ¹³⁶, P. Gordeev ¹⁴⁰, M. Gorgon ², K. Goswami ⁴⁸, S. Gotovac ³³, V. Grabski ⁶⁷, L.K. Graczykowski ¹³⁵, E. Grecka ⁸⁵, A. Grelli ⁵⁹, C. Grigoras ³², V. Grigoriev ¹⁴⁰, S. Grigoryan ^{141,1},

- F. Grossa ³², J.F. Grosse-Oetringhaus ³², R. Grossos ⁹⁶, D. Grund ³⁴, N.A. Grunwald ⁹³,
 G.G. Guardiano ¹¹⁰, R. Guernane ⁷², M. Guilbaud ¹⁰², K. Gulbrandsen ⁸², J.J.W.K. Gumprecht ¹⁰¹,
 T. Gündem ⁶⁴, T. Gunji ¹²³, W. Guo ⁶, A. Gupta ⁹⁰, R. Gupta ⁹⁰, R. Gupta ⁴⁸, K. Gwizdziel ¹³⁵,
 L. Gyulai ⁴⁶, C. Hadjidakis ¹³⁰, F.U. Haider ⁹⁰, S. Haidlova ³⁴, M. Haldar ⁴, H. Hamagaki ⁷⁵,
 Y. Han ¹³⁹, B.G. Hanley ¹³⁶, R. Hannigan ¹⁰⁷, J. Hansen ⁷⁴, M.R. Haque ⁹⁶, J.W. Harris ¹³⁷,
 A. Harton ⁹, M.V. Hartung ⁶⁴, H. Hassan ¹¹⁶, D. Hatzifotiadou ⁵¹, P. Hauer ⁴², L.B. Havener ¹³⁷,
 E. Hellbär ³², H. Helstrup ³⁷, M. Hemmer ⁶⁴, T. Herman ³⁴, S.G. Hernandez ¹¹⁵, G. Herrera Corral ⁸,
 S. Herrmann ¹²⁷, K.F. Hetland ³⁷, B. Heybeck ⁶⁴, H. Hillemanns ³², B. Hippolyte ¹²⁸, I.P.M. Hobus ⁸³,
 F.W. Hoffmann ⁷⁰, B. Hofman ⁵⁹, M. Horst ⁹⁴, A. Horzyk ², Y. Hou ⁶, P. Hristov ³², P. Huhn ⁶⁴,
 L.M. Huhta ¹¹⁶, T.J. Humanic ⁸⁷, A. Hutson ¹¹⁵, D. Hutter ³⁸, M.C. Hwang ¹⁸, R. Ilkaev ¹⁴⁰,
 M. Inaba ¹²⁴, G.M. Innocenti ³², M. Ippolitov ¹⁴⁰, A. Isakov ⁸³, T. Isidori ¹¹⁷, M.S. Islam ^{47,98},
 S. Iurchenko ¹⁴⁰, M. Ivanov ⁹⁶, M. Ivanov ¹³, V. Ivanov ¹⁴⁰, K.E. Iversen ⁷⁴, M. Jablonski ²,
 B. Jacak ^{18,73}, N. Jacazio ²⁵, P.M. Jacobs ⁷³, S. Jadlovská ¹⁰⁵, J. Jadlovsky ¹⁰⁵, S. Jaelani ⁸¹, C. Jahnke ¹⁰⁹,
 M.J. Jakubowska ¹³⁵, M.A. Janik ¹³⁵, T. Janson ⁷⁰, S. Ji ¹⁶, S. Jia ¹⁰, T. Jiang ¹⁰, A.A.P. Jimenez ⁶⁵,
 F. Jonas ⁷³, D.M. Jones ¹¹⁸, J.M. Jowett ^{32,96}, J. Jung ⁶⁴, M. Jung ⁶⁴, A. Junique ³², A. Jusko ⁹⁹,
 J. Kaewjai ¹⁰⁴, P. Kalinak ⁶⁰, A. Kalweit ³², A. Karasu Uysal ¹³⁸, D. Karatovic ⁸⁸, N. Karatzenis ⁹⁹,
 O. Karavichev ¹⁴⁰, T. Karavicheva ¹⁴⁰, E. Karpechev ¹⁴⁰, M.J. Karwowska ¹³⁵, U. Kebschull ⁷⁰,
 M. Keil ³², B. Ketzer ⁴², J. Keul ⁶⁴, S.S. Khade ⁴⁸, A.M. Khan ¹¹⁹, S. Khan ¹⁵, A. Khanzadeev ¹⁴⁰,
 Y. Kharlov ¹⁴⁰, A. Khatun ¹¹⁷, A. Khuntia ³⁴, Z. Khuranova ⁶⁴, B. Kileng ³⁷, B. Kim ¹⁰³, C. Kim ¹⁶,
 D.J. Kim ¹¹⁶, D. Kim ¹⁰³, E.J. Kim ⁶⁹, J. Kim ¹³⁹, J. Kim ⁵⁸, J. Kim ^{32,69}, M. Kim ¹⁸, S. Kim ¹⁷,
 T. Kim ¹³⁹, K. Kimura ⁹¹, A. Kirkova ³⁵, S. Kirsch ⁶⁴, I. Kisiel ³⁸, S. Kiselev ¹⁴⁰, A. Kisiel ¹³⁵,
 J.L. Klay ⁵, J. Klein ³², S. Klein ⁷³, C. Klein-Bösing ¹²⁵, M. Kleiner ⁶⁴, T. Klemenz ⁹⁴, A. Kluge ³²,
 C. Kobdaj ¹⁰⁴, R. Kohara ¹²³, T. Kollegger ⁹⁶, A. Kondratyev ¹⁴¹, N. Kondratyeva ¹⁴⁰, J. Konig ⁶⁴,
 S.A. Konigstorfer ⁹⁴, P.J. Konopka ³², G. Kornakov ¹³⁵, M. Korwieser ⁹⁴, S.D. Koryciak ², C. Koster ⁸³,
 A. Kotliarov ⁸⁵, N. Kovacic ⁸⁸, V. Kovalenko ¹⁴⁰, M. Kowalski ¹⁰⁶, V. Kozhuharov ³⁵, G. Kozlov ³⁸,
 I. Králik ⁶⁰, A. Kravčáková ³⁶, L. Krcal ^{32,38}, M. Krivda ^{99,60}, F. Krizek ⁸⁵, K. Krizkova Gajdosova ³²,
 C. Krug ⁶⁶, M. Krüger ⁶⁴, D.M. Krupova ³⁴, E. Kryshen ¹⁴⁰, V. Kučera ⁵⁸, C. Kuhn ¹²⁸,
 P.G. Kuijer ⁸³, T. Kumaoka ¹²⁴, D. Kumar ¹³⁴, L. Kumar ⁸⁹, N. Kumar ⁸⁹, S. Kumar ⁵⁰, S. Kundu ³²,
 P. Kurashvili ⁷⁸, A.B. Kurepin ¹⁴⁰, A. Kuryakin ¹⁴⁰, S. Kushpil ⁸⁵, V. Kuskov ¹⁴⁰, M. Kutyla ¹³⁵,
 A. Kuznetsov ¹⁴¹, M.J. Kweon ⁵⁸, Y. Kwon ¹³⁹, S.L. La Pointe ³⁸, P. La Rocca ²⁶, A. Lakrathok ¹⁰⁴,
 M. Lamanna ³², A.R. Landou ⁷², R. Langoy ¹²⁰, P. Larionov ³², E. Laudi ³², L. Lautner ⁹⁴,
 R.A.N. Laveaga ¹⁰⁸, R. Lavicka ¹⁰¹, R. Lea ^{133,55}, H. Lee ¹⁰³, I. Legrand ⁴⁵, G. Legras ¹²⁵,
 J. Lehrbach ³⁸, A.M. Lejeune ³⁴, T.M. Lelek ², R.C. Lemmon ^{1,84}, I. León Monzón ¹⁰⁸, M.M. Lesch ⁹⁴,
 P. Lévai ⁴⁶, M. Li ⁶, P. Li ¹⁰, X. Li ¹⁰, B.E. Liang-gilman ¹⁸, J. Lien ¹²⁰, R. Lietava ⁹⁹, I. Likmeta ¹¹⁵,
 B. Lim ²⁴, H. Lim ¹⁶, S.H. Lim ¹⁶, V. Lindenstruth ³⁸, C. Lippmann ⁹⁶, D. Liskova ¹⁰⁵, D.H. Liu ⁶,
 J. Liu ¹¹⁸, G.S.S. Liveraro ¹¹⁰, I.M. Lofnes ²⁰, C. Loizides ⁸⁶, S. Lokos ¹⁰⁶, J. Lömkér ⁵⁹,
 X. Lopez ¹²⁶, E. López Torres ⁷, C. Lotteau ¹²⁷, P. Lu ^{96,119}, Z. Lu ¹⁰, F.V. Lugo ⁶⁷, J.R. Luhder ¹²⁵,
 G. Luparello ⁵⁷, Y.G. Ma ³⁹, M. Mager ³², A. Maire ¹²⁸, E.M. Majerz ², M.V. Makarieva ³⁵,
 M. Malaev ¹⁴⁰, G. Malfattore ²⁵, N.M. Malik ⁹⁰, S.K. Malik ⁹⁰, D. Mallick ¹³⁰, N. Mallick ^{116,48},
 G. Mandaglio ^{30,53}, S.K. Mandal ⁷⁸, A. Manea ⁶³, V. Manko ¹⁴⁰, F. Manso ¹²⁶, V. Manzari ⁵⁰,
 Y. Mao ⁶, R.W. Marcjan ², G.V. Margagliotti ²³, A. Margotti ⁵¹, A. Marín ⁹⁶, C. Markert ¹⁰⁷,
 C.F.B. Marquez ³¹, P. Martinengo ³², M.I. Martínez ⁴⁴, G. Martínez García ¹⁰², M.P.P. Martins ¹⁰⁹,
 S. Masciocchi ⁹⁶, M. Masera ²⁴, A. Masoni ⁵², L. Massacrier ¹³⁰, O. Massen ⁵⁹, A. Mastroserio ^{131,50},
 S. Mattiazzo ²⁷, A. Matyja ¹⁰⁶, F. Mazzaschi ^{32,24}, M. Mazzilli ¹¹⁵, Y. Melikyan ⁴³, M. Melo ¹⁰⁹,
 A. Menchaca-Rocha ⁶⁷, J.E.M. Mendez ⁶⁵, E. Meninno ¹⁰¹, A.S. Menon ¹¹⁵, M.W. Menzel ^{32,93},
 M. Meres ¹³, L. Micheletti ³², D. Mihai ¹¹², D.L. Mihaylov ⁹⁴, K. Mihaylov ^{141,140}, N. Minafra ¹¹⁷,
 D. Miśkowiec ⁹⁶, A. Modak ¹³³, B. Mohanty ⁷⁹, M. Mohisin Khan ^{V,15}, M.A. Molander ⁴³,
 M.M. Mondal ⁷⁹, S. Monira ¹³⁵, C. Mordasini ¹¹⁶, D.A. Moreira De Godoy ¹²⁵, I. Morozov ¹⁴⁰,
 A. Morsch ³², T. Mrnjavac ³², V. Muccifora ⁴⁹, S. Muhuri ¹³⁴, J.D. Mulligan ⁷³, A. Mulliri ²²,
 M.G. Munhoz ¹⁰⁹, R.H. Munzer ⁶⁴, H. Murakami ¹²³, S. Murray ¹¹³, L. Musa ³², J. Musinsky ⁶⁰,
 J.W. Myrcha ¹³⁵, B. Naik ¹²², A.I. Nambrath ¹⁸, B.K. Nandi ⁴⁷, R. Nania ⁵¹, E. Nappi ⁵⁰,
 A.F. Nassirpour ¹⁷, V. Nastase ¹¹², A. Nath ⁹³, S. Nath ¹³⁴, C. Nattrass ¹²¹, M.N. Naydenov ³⁵, A. Neagu ¹⁹,
 A. Negru ¹¹², E. Nekrasova ¹⁴⁰, L. Nellen ⁶⁵, R. Nepeivoda ⁷⁴, S. Nese ¹⁹, N. Nicassio ³¹, B.S. Nielsen ⁸²,
 E.G. Nielsen ⁸², S. Nikolaev ¹⁴⁰, V. Nikulin ¹⁴⁰, F. Noferini ⁵¹, S. Noh ¹², P. Nomokonov ¹⁴¹,
 J. Norman ¹¹⁸, N. Novitzky ⁸⁶, P. Nowakowski ¹³⁵, A. Nyanin ¹⁴⁰, J. Nystrand ²⁰, S. Oh ¹⁷,
 A. Ohlson ⁷⁴, V.A. Okorokov ¹⁴⁰, J. Oleniacz ¹³⁵, A. Onnerstad ¹¹⁶, C. Oppedisano ⁵⁶, A. Ortiz

Velasquez $\text{\textcircled{b}}^{65}$, J. Otwinowski $\text{\textcircled{b}}^{106}$, M. Oya $\text{\textcircled{b}}^{91}$, K. Oyama $\text{\textcircled{b}}^{75}$, S. Padhan $\text{\textcircled{b}}^{47}$, D. Pagano $\text{\textcircled{b}}^{133,55}$, G. Paić $\text{\textcircled{b}}^{65}$, S. Paisano-Guzmán $\text{\textcircled{b}}^{44}$, A. Palasciano $\text{\textcircled{b}}^{50}$, I. Panasenko $\text{\textcircled{b}}^{74}$, S. Panebianco $\text{\textcircled{b}}^{129}$, C. Pantouvakis $\text{\textcircled{b}}^{27}$, H. Park $\text{\textcircled{b}}^{124}$, J. Park $\text{\textcircled{b}}^{124}$, S. Park $\text{\textcircled{b}}^{103}$, J.E. Parkkila $\text{\textcircled{b}}^{32}$, Y. Patley $\text{\textcircled{b}}^{47}$, R.N. Patra $\text{\textcircled{b}}^{50}$, B. Paul $\text{\textcircled{b}}^{134}$, H. Pei $\text{\textcircled{b}}^{6}$, T. Peitzmann $\text{\textcircled{b}}^{59}$, X. Peng $\text{\textcircled{b}}^{11}$, M. Pennisi $\text{\textcircled{b}}^{24}$, S. Perciballi $\text{\textcircled{b}}^{24}$, D. Peresunko $\text{\textcircled{b}}^{140}$, G.M. Perez $\text{\textcircled{b}}^{7}$, Y. Pestov $\text{\textcircled{b}}^{140}$, M.T. Petersen $\text{\textcircled{b}}^{82}$, V. Petrov $\text{\textcircled{b}}^{140}$, M. Petrovici $\text{\textcircled{b}}^{45}$, S. Piano $\text{\textcircled{b}}^{57}$, M. Pikna $\text{\textcircled{b}}^{13}$, P. Pillot $\text{\textcircled{b}}^{102}$, O. Pinazza $\text{\textcircled{b}}^{51,32}$, L. Pinsky $\text{\textcircled{b}}^{115}$, C. Pinto $\text{\textcircled{b}}^{94}$, S. Pisano $\text{\textcircled{b}}^{49}$, M. Płoskoń $\text{\textcircled{b}}^{73}$, M. Planinic $\text{\textcircled{b}}^{88}$, D.K. Plociennik $\text{\textcircled{b}}^{2}$, M.G. Poghosyan $\text{\textcircled{b}}^{86}$, B. Polichtchouk $\text{\textcircled{b}}^{140}$, S. Politano $\text{\textcircled{b}}^{29}$, N. Poljak $\text{\textcircled{b}}^{88}$, A. Pop $\text{\textcircled{b}}^{45}$, S. Porteboeuf-Houssais $\text{\textcircled{b}}^{126}$, V. Pozdniakov $\text{\textcircled{b}}^{1,141}$, I.Y. Pozos $\text{\textcircled{b}}^{44}$, K.K. Pradhan $\text{\textcircled{b}}^{48}$, S.K. Prasad $\text{\textcircled{b}}^{4}$, S. Prasad $\text{\textcircled{b}}^{48}$, R. Preghenella $\text{\textcircled{b}}^{51}$, F. Prino $\text{\textcircled{b}}^{56}$, C.A. Pruneau $\text{\textcircled{b}}^{136}$, I. Pshenichnov $\text{\textcircled{b}}^{140}$, M. Puccio $\text{\textcircled{b}}^{32}$, S. Pucillo $\text{\textcircled{b}}^{24}$, S. Qiu $\text{\textcircled{b}}^{83}$, L. Quaglia $\text{\textcircled{b}}^{24}$, A.M.K. Radhakrishnan $\text{\textcircled{b}}^{48}$, S. Ragoni $\text{\textcircled{b}}^{14}$, A. Rai $\text{\textcircled{b}}^{137}$, A. Rakotozafindrabe $\text{\textcircled{b}}^{129}$, L. Ramello $\text{\textcircled{b}}^{132,56}$, M. Rasa $\text{\textcircled{b}}^{26}$, S.S. Räsänen $\text{\textcircled{b}}^{43}$, R. Rath $\text{\textcircled{b}}^{51}$, M.P. Rauch $\text{\textcircled{b}}^{20}$, I. Ravasenga $\text{\textcircled{b}}^{32}$, K.F. Read $\text{\textcircled{b}}^{86,121}$, C. Reckziegel $\text{\textcircled{b}}^{111}$, A.R. Redelbach $\text{\textcircled{b}}^{38}$, K. Redlich $\text{\textcircled{b}}^{\text{VI},78}$, C.A. Reetz $\text{\textcircled{b}}^{96}$, H.D. Regules-Medel $\text{\textcircled{b}}^{44}$, A. Rehman $\text{\textcircled{b}}^{20}$, F. Reidt $\text{\textcircled{b}}^{32}$, H.A. Reme-Ness $\text{\textcircled{b}}^{37}$, K. Reygers $\text{\textcircled{b}}^{93}$, A. Riabov $\text{\textcircled{b}}^{140}$, V. Riabov $\text{\textcircled{b}}^{140}$, R. Ricci $\text{\textcircled{b}}^{28}$, M. Richter $\text{\textcircled{b}}^{20}$, A.A. Riedel $\text{\textcircled{b}}^{94}$, W. Riegler $\text{\textcircled{b}}^{32}$, A.G. Riffero $\text{\textcircled{b}}^{24}$, M. Rignanese $\text{\textcircled{b}}^{27}$, C. Ripoli $\text{\textcircled{b}}^{28}$, C. Ristea $\text{\textcircled{b}}^{63}$, M.V. Rodriguez $\text{\textcircled{b}}^{32}$, M. Rodríguez Cahuantzi $\text{\textcircled{b}}^{44}$, S.A. Rodríguez Ramírez $\text{\textcircled{b}}^{44}$, K. Røed $\text{\textcircled{b}}^{19}$, R. Rogalev $\text{\textcircled{b}}^{140}$, E. Rogochaya $\text{\textcircled{b}}^{141}$, T.S. Rogoschinski $\text{\textcircled{b}}^{64}$, D. Rohr $\text{\textcircled{b}}^{32}$, D. Röhrich $\text{\textcircled{b}}^{20}$, S. Rojas Torres $\text{\textcircled{b}}^{34}$, P.S. Rokita $\text{\textcircled{b}}^{135}$, G. Romanenko $\text{\textcircled{b}}^{25}$, F. Ronchetti $\text{\textcircled{b}}^{32}$, E.D. Rosas $\text{\textcircled{b}}^{65}$, K. Roslon $\text{\textcircled{b}}^{135}$, A. Rossi $\text{\textcircled{b}}^{54}$, A. Roy $\text{\textcircled{b}}^{48}$, S. Roy $\text{\textcircled{b}}^{47}$, N. Rubini $\text{\textcircled{b}}^{51,25}$, J.A. Rudolph $\text{\textcircled{b}}^{83}$, D. Ruggiano $\text{\textcircled{b}}^{135}$, R. Rui $\text{\textcircled{b}}^{23}$, P.G. Russek $\text{\textcircled{b}}^2$, R. Russo $\text{\textcircled{b}}^{83}$, A. Rustamov $\text{\textcircled{b}}^{80}$, E. Ryabinkin $\text{\textcircled{b}}^{140}$, Y. Ryabov $\text{\textcircled{b}}^{140}$, A. Rybicki $\text{\textcircled{b}}^{106}$, J. Ryu $\text{\textcircled{b}}^{16}$, W. Rzesz $\text{\textcircled{b}}^{135}$, B. Sabiu $\text{\textcircled{b}}^{51}$, S. Sadovsky $\text{\textcircled{b}}^{140}$, J. Saetre $\text{\textcircled{b}}^{20}$, S. Saha $\text{\textcircled{b}}^{79}$, B. Sahoo $\text{\textcircled{b}}^{48}$, R. Sahoo $\text{\textcircled{b}}^{48}$, S. Sahoo $\text{\textcircled{b}}^{61}$, D. Sahu $\text{\textcircled{b}}^{48}$, P.K. Sahu $\text{\textcircled{b}}^{61}$, J. Saini $\text{\textcircled{b}}^{134}$, K. Sajdakova $\text{\textcircled{b}}^{36}$, S. Sakai $\text{\textcircled{b}}^{124}$, M.P. Salvan $\text{\textcircled{b}}^{96}$, S. Sambyal $\text{\textcircled{b}}^{90}$, D. Samitz $\text{\textcircled{b}}^{101}$, I. Sanna $\text{\textcircled{b}}^{32,94}$, T.B. Saramela $\text{\textcircled{b}}^{109}$, D. Sarkar $\text{\textcircled{b}}^{82}$, P. Sarma $\text{\textcircled{b}}^{41}$, V. Sarritzu $\text{\textcircled{b}}^{22}$, V.M. Sarti $\text{\textcircled{b}}^{94}$, M.H.P. Sas $\text{\textcircled{b}}^{32}$, S. Sawan $\text{\textcircled{b}}^{79}$, E. Scapparone $\text{\textcircled{b}}^{51}$, J. Schambach $\text{\textcircled{b}}^{86}$, H.S. Scheid $\text{\textcircled{b}}^{64}$, C. Schiaua $\text{\textcircled{b}}^{45}$, R. Schicker $\text{\textcircled{b}}^{93}$, F. Schlepper $\text{\textcircled{b}}^{93}$, A. Schmah $\text{\textcircled{b}}^{96}$, C. Schmidt $\text{\textcircled{b}}^{96}$, M.O. Schmidt $\text{\textcircled{b}}^{32}$, M. Schmidt $\text{\textcircled{b}}^{92}$, N.V. Schmidt $\text{\textcircled{b}}^{86}$, A.R. Schmier $\text{\textcircled{b}}^{121}$, J. Schoengarth $\text{\textcircled{b}}^{64}$, R. Schotter $\text{\textcircled{b}}^{101,128}$, A. Schröter $\text{\textcircled{b}}^{38}$, J. Schukraft $\text{\textcircled{b}}^{32}$, K. Schweda $\text{\textcircled{b}}^{96}$, G. Scioli $\text{\textcircled{b}}^{25}$, E. Scomparin $\text{\textcircled{b}}^{56}$, J.E. Seger $\text{\textcircled{b}}^{14}$, Y. Sekiguchi $\text{\textcircled{b}}^{123}$, D. Sekihata $\text{\textcircled{b}}^{123}$, M. Selina $\text{\textcircled{b}}^{83}$, I. Selyuzhenkov $\text{\textcircled{b}}^{96}$, S. Senyukov $\text{\textcircled{b}}^{128}$, J.J. Seo $\text{\textcircled{b}}^{93}$, D. Serebryakov $\text{\textcircled{b}}^{140}$, L. Serkin $\text{\textcircled{b}}^{\text{VII},65}$, L. Šerkšnyté $\text{\textcircled{b}}^{94}$, A. Sevcenco $\text{\textcircled{b}}^{63}$, T.J. Shaba $\text{\textcircled{b}}^{68}$, A. Shabetai $\text{\textcircled{b}}^{102}$, R. Shahoyan $\text{\textcircled{b}}^{32}$, A. Shangaraev $\text{\textcircled{b}}^{140}$, B. Sharma $\text{\textcircled{b}}^{90}$, D. Sharma $\text{\textcircled{b}}^{47}$, H. Sharma $\text{\textcircled{b}}^{54}$, M. Sharma $\text{\textcircled{b}}^{90}$, S. Sharma $\text{\textcircled{b}}^{75}$, S. Sharma $\text{\textcircled{b}}^{90}$, U. Sharma $\text{\textcircled{b}}^{90}$, A. Shatat $\text{\textcircled{b}}^{130}$, O. Sheibani $\text{\textcircled{b}}^{136,115}$, K. Shigaki $\text{\textcircled{b}}^{91}$, M. Shimomura $\text{\textcircled{b}}^{76}$, J. Shin $\text{\textcircled{b}}^{12}$, S. Shirinkin $\text{\textcircled{b}}^{140}$, Q. Shou $\text{\textcircled{b}}^{39}$, Y. Sibiriak $\text{\textcircled{b}}^{140}$, S. Siddhanta $\text{\textcircled{b}}^{52}$, T. Siemiaczuk $\text{\textcircled{b}}^{78}$, T.F. Silva $\text{\textcircled{b}}^{109}$, D. Silvermyr $\text{\textcircled{b}}^{74}$, T. Simantathammakul $\text{\textcircled{b}}^{104}$, R. Simeonov $\text{\textcircled{b}}^{35}$, B. Singh $\text{\textcircled{b}}^{90}$, B. Singh $\text{\textcircled{b}}^{94}$, K. Singh $\text{\textcircled{b}}^{48}$, R. Singh $\text{\textcircled{b}}^{79}$, R. Singh $\text{\textcircled{b}}^{90}$, R. Singh $\text{\textcircled{b}}^{54,96}$, S. Singh $\text{\textcircled{b}}^{15}$, V.K. Singh $\text{\textcircled{b}}^{134}$, V. Singhal $\text{\textcircled{b}}^{134}$, T. Sinha $\text{\textcircled{b}}^{98}$, B. Sitar $\text{\textcircled{b}}^{13}$, M. Sitta $\text{\textcircled{b}}^{132,56}$, T.B. Skaali $\text{\textcircled{b}}^{19}$, G. Skorodumovs $\text{\textcircled{b}}^{93}$, N. Smirnov $\text{\textcircled{b}}^{137}$, R.J.M. Snellings $\text{\textcircled{b}}^{59}$, E.H. Solheim $\text{\textcircled{b}}^{19}$, C. Sonnabend $\text{\textcircled{b}}^{32,96}$, J.M. Sonneveld $\text{\textcircled{b}}^{83}$, F. Soramel $\text{\textcircled{b}}^{27}$, A.B. Soto-hernandez $\text{\textcircled{b}}^{87}$, R. Spijkers $\text{\textcircled{b}}^{83}$, I. Sputowska $\text{\textcircled{b}}^{106}$, J. Staa $\text{\textcircled{b}}^{74}$, J. Stachel $\text{\textcircled{b}}^{93}$, I. Stan $\text{\textcircled{b}}^{63}$, P.J. Steffanic $\text{\textcircled{b}}^{121}$, T. Stellhorn $\text{\textcircled{b}}^{125}$, S.F. Stiefelmaier $\text{\textcircled{b}}^{93}$, D. Stocco $\text{\textcircled{b}}^{102}$, I. Storehaug $\text{\textcircled{b}}^{19}$, N.J. Strangmann $\text{\textcircled{b}}^{64}$, P. Stratmann $\text{\textcircled{b}}^{125}$, S. Strazzi $\text{\textcircled{b}}^{25}$, A. Sturniolo $\text{\textcircled{b}}^{30,53}$, C.P. Stylianidis $\text{\textcircled{b}}^{83}$, A.A.P. Suaide $\text{\textcircled{b}}^{109}$, C. Suire $\text{\textcircled{b}}^{130}$, A. Suiu $\text{\textcircled{b}}^{32,112}$, M. Sukhanov $\text{\textcircled{b}}^{140}$, M. Suljic $\text{\textcircled{b}}^{32}$, R. Sultanov $\text{\textcircled{b}}^{140}$, V. Sumberia $\text{\textcircled{b}}^{90}$, S. Sumowidagdo $\text{\textcircled{b}}^{81}$, L.H. Tabares $\text{\textcircled{b}}^7$, S.F. Taghavi $\text{\textcircled{b}}^{94}$, J. Takahashi $\text{\textcircled{b}}^{110}$, G.J. Tambave $\text{\textcircled{b}}^{79}$, S. Tang $\text{\textcircled{b}}^6$, Z. Tang $\text{\textcircled{b}}^{119}$, J.D. Tapia Takaki $\text{\textcircled{b}}^{117}$, N. Tapus $\text{\textcircled{b}}^{112}$, L.A. Tarasovicova $\text{\textcircled{b}}^{36}$, M.G. Tarzila $\text{\textcircled{b}}^{45}$, A. Tauro $\text{\textcircled{b}}^{32}$, A. Tavira García $\text{\textcircled{b}}^{130}$, G. Tejeda Muñoz $\text{\textcircled{b}}^{44}$, L. Terlizzi $\text{\textcircled{b}}^{24}$, C. Terrevoli $\text{\textcircled{b}}^{50}$, S. Thakur $\text{\textcircled{b}}^4$, M. Thogersen $\text{\textcircled{b}}^{19}$, D. Thomas $\text{\textcircled{b}}^{107}$, A. Tikhonov $\text{\textcircled{b}}^{140}$, N. Tiltmann $\text{\textcircled{b}}^{32,125}$, A.R. Timmins $\text{\textcircled{b}}^{115}$, M. Tkacik $\text{\textcircled{b}}^{105}$, T. Tkacik $\text{\textcircled{b}}^{105}$, A. Toia $\text{\textcircled{b}}^{64}$, R. Tokumoto $\text{\textcircled{b}}^{91}$, S. Tomassini $\text{\textcircled{b}}^{25}$, K. Tomohiro $\text{\textcircled{b}}^{91}$, N. Topilskaya $\text{\textcircled{b}}^{140}$, M. Toppi $\text{\textcircled{b}}^{49}$, V.V. Torres $\text{\textcircled{b}}^{102}$, A.G. Torres Ramos $\text{\textcircled{b}}^{31}$, A. Trifirò $\text{\textcircled{b}}^{30,53}$, T. Triloki $\text{\textcircled{b}}^{95}$, A.S. Triolo $\text{\textcircled{b}}^{32,30,53}$, S. Tripathy $\text{\textcircled{b}}^{32}$, T. Tripathy $\text{\textcircled{b}}^{126,47}$, S. Trogolo $\text{\textcircled{b}}^{24}$, V. Trubnikov $\text{\textcircled{b}}^3$, W.H. Trzaska $\text{\textcircled{b}}^{116}$, T.P. Trzcinski $\text{\textcircled{b}}^{135}$, C. Tsolanta $\text{\textcircled{b}}^{19}$, R. Tu $\text{\textcircled{b}}^{39}$, A. Tumkin $\text{\textcircled{b}}^{140}$, R. Turrisi $\text{\textcircled{b}}^{54}$, T.S. Tveter $\text{\textcircled{b}}^{19}$, K. Ullaland $\text{\textcircled{b}}^{20}$, B. Ulukutlu $\text{\textcircled{b}}^{94}$, S. Upadhyaya $\text{\textcircled{b}}^{106}$, A. Uras $\text{\textcircled{b}}^{127}$, G.L. Usai $\text{\textcircled{b}}^{22}$, M. Vala $\text{\textcircled{b}}^{36}$, N. Valle $\text{\textcircled{b}}^{55}$, L.V.R. van Doremalen $\text{\textcircled{b}}^{59}$, M. van Leeuwen $\text{\textcircled{b}}^{83}$, C.A. van Veen $\text{\textcircled{b}}^{93}$, R.J.G. van Weelden $\text{\textcircled{b}}^{83}$, P. Vande Vyvre $\text{\textcircled{b}}^{32}$, D. Varga $\text{\textcircled{b}}^{46}$, Z. Varga $\text{\textcircled{b}}^{137,46}$, P. Vargas Torres $\text{\textcircled{b}}^{65}$, M. Vasileiou $\text{\textcircled{b}}^{77}$, A. Vasiliev $\text{\textcircled{b}}^{1,140}$, O. Vázquez Doce $\text{\textcircled{b}}^{49}$, O. Vazquez Rueda $\text{\textcircled{b}}^{115}$, V. Vechernin $\text{\textcircled{b}}^{140}$, E. Vercellin $\text{\textcircled{b}}^{24}$, R. Verma $\text{\textcircled{b}}^{47}$, R. Vértesi $\text{\textcircled{b}}^{46}$, M. Verweij $\text{\textcircled{b}}^{59}$, L. Vickovic $\text{\textcircled{b}}^{33}$, Z. Vilakazi $\text{\textcircled{b}}^{122}$, O. Villalobos Baillie $\text{\textcircled{b}}^{99}$, A. Villani $\text{\textcircled{b}}^{23}$, A. Vinogradov $\text{\textcircled{b}}^{140}$, T. Virgili $\text{\textcircled{b}}^{28}$, M.M.O. Virta $\text{\textcircled{b}}^{116}$, A. Vodopyanov $\text{\textcircled{b}}^{141}$, B. Volkel $\text{\textcircled{b}}^{32}$, M.A. Völkli $\text{\textcircled{b}}^{93}$, S.A. Voloshin $\text{\textcircled{b}}^{136}$, G. Volpe $\text{\textcircled{b}}^{31}$, B. von Haller $\text{\textcircled{b}}^{32}$, I. Vorobyev $\text{\textcircled{b}}^{32}$, N. Vozniuk $\text{\textcircled{b}}^{140}$, J. Vrláková $\text{\textcircled{b}}^{36}$, J. Wan $\text{\textcircled{b}}^{39}$, C. Wang $\text{\textcircled{b}}^{39}$, D. Wang $\text{\textcircled{b}}^{39}$, Y. Wang $\text{\textcircled{b}}^{39}$, Y. Wang $\text{\textcircled{b}}^6$, Z. Wang $\text{\textcircled{b}}^{39}$, A. Wegrzynek $\text{\textcircled{b}}^{32}$, F.T. Weiglhofer $\text{\textcircled{b}}^{38}$, S.C. Wenzel $\text{\textcircled{b}}^{32}$, J.P. Wessels $\text{\textcircled{b}}^{125}$, P.K. Wiacek $\text{\textcircled{b}}^2$, J. Wiechula $\text{\textcircled{b}}^{64}$, J. Wikne $\text{\textcircled{b}}^{19}$, G. Wilk $\text{\textcircled{b}}^{78}$, J. Wilkinson $\text{\textcircled{b}}^{96}$,

G.A. Willems ¹²⁵, B. Windelband ⁹³, M. Winn ¹²⁹, J.R. Wright ¹⁰⁷, W. Wu ³⁹, Y. Wu ¹¹⁹, Z. Xiong ¹¹⁹, R. Xu ⁶, A. Yadav ⁴², A.K. Yadav ¹³⁴, Y. Yamaguchi ⁹¹, S. Yang ²⁰, S. Yano ⁹¹, E.R. Yeats ¹⁸, Z. Yin ⁶, I.-K. Yoo ¹⁶, J.H. Yoon ⁵⁸, H. Yu ¹², S. Yuan ²⁰, A. Yuncu ⁹³, V. Zaccolo ²³, C. Zampolli ³², F. Zanone ⁹³, N. Zardoshti ³², A. Zarochentsev ¹⁴⁰, P. Závada ⁶², N. Zaviyalov ¹⁴⁰, M. Zhalov ¹⁴⁰, B. Zhang ^{93,6}, C. Zhang ¹²⁹, L. Zhang ³⁹, M. Zhang ^{126,6}, M. Zhang ⁶, S. Zhang ³⁹, X. Zhang ⁶, Y. Zhang ¹¹⁹, Z. Zhang ⁶, M. Zhao ¹⁰, V. Zhrebchevskii ¹⁴⁰, Y. Zhi ¹⁰, D. Zhou ⁶, Y. Zhou ⁸², J. Zhu ^{54,6}, S. Zhu ¹¹⁹, Y. Zhu ⁶, S.C. Zugravel ⁵⁶, N. Zurlo ^{133,55}

Affiliation Notes

^I Deceased

^{II} Also at: Max-Planck-Institut fur Physik, Munich, Germany

^{III} Also at: Italian National Agency for New Technologies, Energy and Sustainable Economic Development (ENEA), Bologna, Italy

^{IV} Also at: Dipartimento DET del Politecnico di Torino, Turin, Italy

^V Also at: Department of Applied Physics, Aligarh Muslim University, Aligarh, India

^{VI} Also at: Institute of Theoretical Physics, University of Wroclaw, Poland

^{VII} Also at: Facultad de Ciencias, Universidad Nacional Autónoma de México, Mexico City, Mexico

Collaboration Institutes

¹ A.I. Alikhanyan National Science Laboratory (Yerevan Physics Institute) Foundation, Yerevan, Armenia

² AGH University of Krakow, Cracow, Poland

³ Bogolyubov Institute for Theoretical Physics, National Academy of Sciences of Ukraine, Kiev, Ukraine

⁴ Bose Institute, Department of Physics and Centre for Astroparticle Physics and Space Science (CAPSS), Kolkata, India

⁵ California Polytechnic State University, San Luis Obispo, California, United States

⁶ Central China Normal University, Wuhan, China

⁷ Centro de Aplicaciones Tecnológicas y Desarrollo Nuclear (CEADEN), Havana, Cuba

⁸ Centro de Investigación y de Estudios Avanzados (CINVESTAV), Mexico City and Mérida, Mexico

⁹ Chicago State University, Chicago, Illinois, United States

¹⁰ China Institute of Atomic Energy, Beijing, China

¹¹ China University of Geosciences, Wuhan, China

¹² Chungbuk National University, Cheongju, Republic of Korea

¹³ Comenius University Bratislava, Faculty of Mathematics, Physics and Informatics, Bratislava, Slovak Republic

¹⁴ Creighton University, Omaha, Nebraska, United States

¹⁵ Department of Physics, Aligarh Muslim University, Aligarh, India

¹⁶ Department of Physics, Pusan National University, Pusan, Republic of Korea

¹⁷ Department of Physics, Sejong University, Seoul, Republic of Korea

¹⁸ Department of Physics, University of California, Berkeley, California, United States

¹⁹ Department of Physics, University of Oslo, Oslo, Norway

²⁰ Department of Physics and Technology, University of Bergen, Bergen, Norway

²¹ Dipartimento di Fisica, Università di Pavia, Pavia, Italy

²² Dipartimento di Fisica dell'Università and Sezione INFN, Cagliari, Italy

²³ Dipartimento di Fisica dell'Università and Sezione INFN, Trieste, Italy

²⁴ Dipartimento di Fisica dell'Università and Sezione INFN, Turin, Italy

²⁵ Dipartimento di Fisica e Astronomia dell'Università and Sezione INFN, Bologna, Italy

²⁶ Dipartimento di Fisica e Astronomia dell'Università and Sezione INFN, Catania, Italy

²⁷ Dipartimento di Fisica e Astronomia dell'Università and Sezione INFN, Padova, Italy

²⁸ Dipartimento di Fisica 'E.R. Caianiello' dell'Università and Gruppo Collegato INFN, Salerno, Italy

²⁹ Dipartimento DISAT del Politecnico and Sezione INFN, Turin, Italy

³⁰ Dipartimento di Scienze MIFT, Università di Messina, Messina, Italy

³¹ Dipartimento Interateneo di Fisica 'M. Merlin' and Sezione INFN, Bari, Italy

³² European Organization for Nuclear Research (CERN), Geneva, Switzerland

³³ Faculty of Electrical Engineering, Mechanical Engineering and Naval Architecture, University of Split, Split, Croatia

- ³⁴ Faculty of Nuclear Sciences and Physical Engineering, Czech Technical University in Prague, Prague, Czech Republic
- ³⁵ Faculty of Physics, Sofia University, Sofia, Bulgaria
- ³⁶ Faculty of Science, P.J. Šafárik University, Košice, Slovak Republic
- ³⁷ Faculty of Technology, Environmental and Social Sciences, Bergen, Norway
- ³⁸ Frankfurt Institute for Advanced Studies, Johann Wolfgang Goethe-Universität Frankfurt, Frankfurt, Germany
- ³⁹ Fudan University, Shanghai, China
- ⁴⁰ Gangneung-Wonju National University, Gangneung, Republic of Korea
- ⁴¹ Gauhati University, Department of Physics, Guwahati, India
- ⁴² Helmholtz-Institut für Strahlen- und Kernphysik, Rheinische Friedrich-Wilhelms-Universität Bonn, Bonn, Germany
- ⁴³ Helsinki Institute of Physics (HIP), Helsinki, Finland
- ⁴⁴ High Energy Physics Group, Universidad Autónoma de Puebla, Puebla, Mexico
- ⁴⁵ Horia Hulubei National Institute of Physics and Nuclear Engineering, Bucharest, Romania
- ⁴⁶ HUN-REN Wigner Research Centre for Physics, Budapest, Hungary
- ⁴⁷ Indian Institute of Technology Bombay (IIT), Mumbai, India
- ⁴⁸ Indian Institute of Technology Indore, Indore, India
- ⁴⁹ INFN, Laboratori Nazionali di Frascati, Frascati, Italy
- ⁵⁰ INFN, Sezione di Bari, Bari, Italy
- ⁵¹ INFN, Sezione di Bologna, Bologna, Italy
- ⁵² INFN, Sezione di Cagliari, Cagliari, Italy
- ⁵³ INFN, Sezione di Catania, Catania, Italy
- ⁵⁴ INFN, Sezione di Padova, Padova, Italy
- ⁵⁵ INFN, Sezione di Pavia, Pavia, Italy
- ⁵⁶ INFN, Sezione di Torino, Turin, Italy
- ⁵⁷ INFN, Sezione di Trieste, Trieste, Italy
- ⁵⁸ Inha University, Incheon, Republic of Korea
- ⁵⁹ Institute for Gravitational and Subatomic Physics (GRASP), Utrecht University/Nikhef, Utrecht, Netherlands
- ⁶⁰ Institute of Experimental Physics, Slovak Academy of Sciences, Košice, Slovak Republic
- ⁶¹ Institute of Physics, Homi Bhabha National Institute, Bhubaneswar, India
- ⁶² Institute of Physics of the Czech Academy of Sciences, Prague, Czech Republic
- ⁶³ Institute of Space Science (ISS), Bucharest, Romania
- ⁶⁴ Institut für Kernphysik, Johann Wolfgang Goethe-Universität Frankfurt, Frankfurt, Germany
- ⁶⁵ Instituto de Ciencias Nucleares, Universidad Nacional Autónoma de México, Mexico City, Mexico
- ⁶⁶ Instituto de Física, Universidade Federal do Rio Grande do Sul (UFRGS), Porto Alegre, Brazil
- ⁶⁷ Instituto de Física, Universidad Nacional Autónoma de México, Mexico City, Mexico
- ⁶⁸ iThemba LABS, National Research Foundation, Somerset West, South Africa
- ⁶⁹ Jeonbuk National University, Jeonju, Republic of Korea
- ⁷⁰ Johann-Wolfgang-Goethe Universität Frankfurt Institut für Informatik, Fachbereich Informatik und Mathematik, Frankfurt, Germany
- ⁷¹ Korea Institute of Science and Technology Information, Daejeon, Republic of Korea
- ⁷² Laboratoire de Physique Subatomique et de Cosmologie, Université Grenoble-Alpes, CNRS-IN2P3, Grenoble, France
- ⁷³ Lawrence Berkeley National Laboratory, Berkeley, California, United States
- ⁷⁴ Lund University Department of Physics, Division of Particle Physics, Lund, Sweden
- ⁷⁵ Nagasaki Institute of Applied Science, Nagasaki, Japan
- ⁷⁶ Nara Women's University (NWU), Nara, Japan
- ⁷⁷ National and Kapodistrian University of Athens, School of Science, Department of Physics , Athens, Greece
- ⁷⁸ National Centre for Nuclear Research, Warsaw, Poland
- ⁷⁹ National Institute of Science Education and Research, Homi Bhabha National Institute, Jatni, India
- ⁸⁰ National Nuclear Research Center, Baku, Azerbaijan
- ⁸¹ National Research and Innovation Agency - BRIN, Jakarta, Indonesia
- ⁸² Niels Bohr Institute, University of Copenhagen, Copenhagen, Denmark
- ⁸³ Nikhef, National institute for subatomic physics, Amsterdam, Netherlands
- ⁸⁴ Nuclear Physics Group, STFC Daresbury Laboratory, Daresbury, United Kingdom
- ⁸⁵ Nuclear Physics Institute of the Czech Academy of Sciences, Husinec-Řež, Czech Republic

- ⁸⁶ Oak Ridge National Laboratory, Oak Ridge, Tennessee, United States
⁸⁷ Ohio State University, Columbus, Ohio, United States
⁸⁸ Physics department, Faculty of science, University of Zagreb, Zagreb, Croatia
⁸⁹ Physics Department, Panjab University, Chandigarh, India
⁹⁰ Physics Department, University of Jammu, Jammu, India
⁹¹ Physics Program and International Institute for Sustainability with Knotted Chiral Meta Matter (WPI-SKCM²), Hiroshima University, Hiroshima, Japan
⁹² Physikalischs Institut, Eberhard-Karls-Universität Tübingen, Tübingen, Germany
⁹³ Physikalischs Institut, Ruprecht-Karls-Universität Heidelberg, Heidelberg, Germany
⁹⁴ Physik Department, Technische Universität München, Munich, Germany
⁹⁵ Politecnico di Bari and Sezione INFN, Bari, Italy
⁹⁶ Research Division and ExtreMe Matter Institute EMMI, GSI Helmholtzzentrum für Schwerionenforschung GmbH, Darmstadt, Germany
⁹⁷ Saga University, Saga, Japan
⁹⁸ Saha Institute of Nuclear Physics, Homi Bhabha National Institute, Kolkata, India
⁹⁹ School of Physics and Astronomy, University of Birmingham, Birmingham, United Kingdom
¹⁰⁰ Sección Física, Departamento de Ciencias, Pontificia Universidad Católica del Perú, Lima, Peru
¹⁰¹ Stefan Meyer Institut für Subatomare Physik (SMI), Vienna, Austria
¹⁰² SUBATECH, IMT Atlantique, Nantes Université, CNRS-IN2P3, Nantes, France
¹⁰³ Sungkyunkwan University, Suwon City, Republic of Korea
¹⁰⁴ Suranaree University of Technology, Nakhon Ratchasima, Thailand
¹⁰⁵ Technical University of Košice, Košice, Slovak Republic
¹⁰⁶ The Henryk Niewodniczanski Institute of Nuclear Physics, Polish Academy of Sciences, Cracow, Poland
¹⁰⁷ The University of Texas at Austin, Austin, Texas, United States
¹⁰⁸ Universidad Autónoma de Sinaloa, Culiacán, Mexico
¹⁰⁹ Universidade de São Paulo (USP), São Paulo, Brazil
¹¹⁰ Universidade Estadual de Campinas (UNICAMP), Campinas, Brazil
¹¹¹ Universidade Federal do ABC, Santo Andre, Brazil
¹¹² Universitatea Nationala de Stiinta si Tehnologie Politehnica Bucuresti, Bucharest, Romania
¹¹³ University of Cape Town, Cape Town, South Africa
¹¹⁴ University of Derby, Derby, United Kingdom
¹¹⁵ University of Houston, Houston, Texas, United States
¹¹⁶ University of Jyväskylä, Jyväskylä, Finland
¹¹⁷ University of Kansas, Lawrence, Kansas, United States
¹¹⁸ University of Liverpool, Liverpool, United Kingdom
¹¹⁹ University of Science and Technology of China, Hefei, China
¹²⁰ University of South-Eastern Norway, Kongsberg, Norway
¹²¹ University of Tennessee, Knoxville, Tennessee, United States
¹²² University of the Witwatersrand, Johannesburg, South Africa
¹²³ University of Tokyo, Tokyo, Japan
¹²⁴ University of Tsukuba, Tsukuba, Japan
¹²⁵ Universität Münster, Institut für Kernphysik, Münster, Germany
¹²⁶ Université Clermont Auvergne, CNRS/IN2P3, LPC, Clermont-Ferrand, France
¹²⁷ Université de Lyon, CNRS/IN2P3, Institut de Physique des 2 Infinis de Lyon, Lyon, France
¹²⁸ Université de Strasbourg, CNRS, IPHC UMR 7178, F-67000 Strasbourg, France, Strasbourg, France
¹²⁹ Université Paris-Saclay, Centre d'Etudes de Saclay (CEA), IRFU, Département de Physique Nucléaire (DPhN), Saclay, France
¹³⁰ Université Paris-Saclay, CNRS/IN2P3, IJCLab, Orsay, France
¹³¹ Università degli Studi di Foggia, Foggia, Italy
¹³² Università del Piemonte Orientale, Vercelli, Italy
¹³³ Università di Brescia, Brescia, Italy
¹³⁴ Variable Energy Cyclotron Centre, Homi Bhabha National Institute, Kolkata, India
¹³⁵ Warsaw University of Technology, Warsaw, Poland
¹³⁶ Wayne State University, Detroit, Michigan, United States
¹³⁷ Yale University, New Haven, Connecticut, United States
¹³⁸ Yildiz Technical University, Istanbul, Turkey

¹³⁹ Yonsei University, Seoul, Republic of Korea

¹⁴⁰ Affiliated with an institute covered by a cooperation agreement with CERN

¹⁴¹ Affiliated with an international laboratory covered by a cooperation agreement with CERN.